



HAL
open science

Disruption of the coxsackievirus and adenovirus receptor- homodimeric interaction triggers lipid microdomain- and dynamin-dependent endocytosis and lysosomal targeting

S. Salinas, C. Zussy, F. Loustalot, D. Henaff, G. Menendez, P. E. Morton, M. Parsons, G. Schiavo, E. J. Kremer

► To cite this version:

S. Salinas, C. Zussy, F. Loustalot, D. Henaff, G. Menendez, et al.. Disruption of the coxsackievirus and adenovirus receptor- homodimeric interaction triggers lipid microdomain- and dynamin-dependent endocytosis and lysosomal targeting. *Journal of Biological Chemistry*, 2013, 10.1074/jbc.M113.518365 . hal-02193683

HAL Id: hal-02193683

<https://hal.science/hal-02193683>

Submitted on 15 Oct 2020

HAL is a multi-disciplinary open access archive for the deposit and dissemination of scientific research documents, whether they are published or not. The documents may come from teaching and research institutions in France or abroad, or from public or private research centers.

L'archive ouverte pluridisciplinaire **HAL**, est destinée au dépôt et à la diffusion de documents scientifiques de niveau recherche, publiés ou non, émanant des établissements d'enseignement et de recherche français ou étrangers, des laboratoires publics ou privés.



Distributed under a Creative Commons Attribution 4.0 International License

Disruption of the Coxsackievirus and Adenovirus Receptor-Homodimeric Interaction Triggers Lipid Microdomain- and Dynamin-dependent Endocytosis and Lysosomal Targeting*

Received for publication, September 12, 2013, and in revised form, November 18, 2013. Published, JBC Papers in Press, November 22, 2013, DOI 10.1074/jbc.M113.518365

Sara Salinas^{†1,2,3}, Charleine Zussy^{†1}, Fabien Loustalot[‡], Daniel Henaff[‡], Guillermo Menendez^{§4}, Penny E. Morton^{¶1}, Maddy Parsons^{¶1}, Giampietro Schiavo^{§4,5}, and Eric J. Kremer^{‡2,6}

From the [†]Institut de Génétique Moléculaire de Montpellier, CNRS UMR 5535, Montpellier, Universités de Montpellier I & II, Montpellier, France, the [¶]Randall Division of Cell and Molecular Biophysics, Kings College London, New Hunts House, Guys Campus, London, United Kingdom, and the [§]Molecular NeuroPathobiology Laboratory, Cancer Research UK London Research Institute, London, United Kingdom

Background: The coxsackievirus and adenovirus receptor (CAR) acts as a docking factor during infection.

Results: Adenovirus fiber knob induces CAR internalization via a pathway involving lipid microdomain integrity, actin dynamics, and dynamin.

Conclusion: In neurons, CAR is linked to endocytic pathways that could modulate its function or regulate viral infection.

Significance: Learning how viruses use receptors to enter and spread in the nervous system.

The coxsackievirus and adenovirus receptor (CAR) serves as a docking factor for some adenovirus (AdV) types and group B coxsackieviruses. Its role in AdV internalization is unclear as studies suggest that its intracellular domain is dispensable for some AdV infection. We previously showed that in motor neurons, AdV induced CAR internalization and co-transport in axons, suggesting that CAR was linked to endocytic and long-range transport machineries. Here, we characterized the mechanisms of CAR endocytosis in neurons and neuronal cells. We found that CAR internalization was lipid microdomain-, actin-, and dynamin-dependent, and subsequently followed by CAR degradation in lysosomes. Moreover, ligands that disrupted the homodimeric CAR interactions in its D1 domains triggered an internalization cascade involving sequences in its intracellular tail.

Cell surface molecules are often responsible for the initial recognition of pathogens by the host, and thus much effort has been devoted to characterize how cells capture pathogens. In the nervous system, several cell adhesion molecules (CAMs)⁷

located at nerve terminals bind viruses, including members of *Herpesviridae* and *Picornaviridae* (1). Virus propagation and/or latency depend on their ability to be internalized and to recruit the axonal transport machinery to be transported to the cell body of neurons. Axonal transport is a key mechanism in neuronal homeostasis that maintains efficient communication between the somatodendritic compartment and nerve termini. The integrity of this process is crucial for neuronal survival as impairment of factors regulating this pathway can be linked to neurodegenerative disease (2, 3). In this light, viruses are ideal tools to understand cellular processes: for instance, α -herpesvirus and rabies virus have been used as neuronal tracers and to understand signals regulating intracellular trafficking in neurons (1, 4).

The coxsackievirus and adenovirus receptor (CAR, encoded by *CXADR*) is a member of the immunoglobulin (Ig) superfamily (5). It has a single membrane-spanning domain, an extracellular domain of 216 residues composed of two Ig-like domains (D1 and D2), and an intracellular tail composed of 107 residues. The D1 domain can be recognized at the cell surface by many adenovirus (AdV) types and the group B coxsackieviruses (CVB). Our current understanding of its role in AdV entry is that it serves as “docking platform,” but does not significantly participate in internalization. This is based primarily on the finding that when the entire intracellular tail of CAR is deleted AdV infection still progressed efficiently (6). In addition, during CVB entry at tight junctions in epithelial cells, CAR remained at the plasma membrane (7). However, during canine adenovirus type 2 (CAAdV-2, commonly referred as CAV-2) entry in motor neurons, CAR and CAV-2 were co-internalized within axons and transported bidirectionally in pH-neutral endosomes (8). Incubation of motor neurons with recombinant CAV-2 fiber knob

* This work was supported in part by European Community 7th Framework Program FP7/2007–2013 Grant 222992—BrainCAV, the French Agence Nationale de la Recherche, E-Rare, the Fondation de France, the Association pour la Recherche sur la Sclérose Amyotrophique Latérale (ARSLA), and the Association Française contre les Myopathies.

¹ Both authors contributed equally to this work.

² INSERM fellows.

³ To whom correspondence may be addressed. Tel.: 33-4-34-35-96-75; Fax: 33-4-34-35-96-34; E-mail: sara.salinas@igmm.cnrs.fr.

⁴ Supported by Cancer Research UK, Chemical Biology Center, Imperial College London, UK, and the UK Motor Neuron Disease Association.

⁵ Present address: Sobell Dept. of Motor Neuroscience and Movement Disorders, UCL-Institute of Neurology, Queen Square, WC1N 3BG London, United Kingdom.

⁶ To whom correspondence may be addressed. Tel.: 33-4-34-35-96-72; Fax: 33-4-34-35-96-34; E-mail: eric.kremer@igmm.cnrs.fr.

⁷ The abbreviations used are: CAM, cell adhesion molecule; CAR, coxsackievirus and adenovirus receptor; AdV, adenovirus; CVB, group B coxsackievirus; HAdV5, human AdV type 5; CTB, cholera toxin binding fragment; Tf, transferrin; DIV, day *in vitro*; CHC, clathrin heavy chain; MC, microfluidic chamber; Lata, latrunculin A; RFP, red fluorescent protein; FK, fiber knob; pp/c, physical particle per cell.

(FK^{CAV}), which binds in theory three CAR molecules (9), also led to CAR internalization and transport (8). In addition, others have showed that CAR may regulate intracellular signaling pathways through engagement with co-receptors such as junctional adhesion molecule type L (10), or after human AdV type 5 (HAdV5) binding (11). Interestingly, HAdV5 FK was efficiently internalized in lacrimal acinar cells and may stimulate endocytic pathways such as macropinocytosis to regulate HAdV5 entry (12). Whether this effect was CAR-dependent was, however, not addressed.

CAMs and other receptors respond to external cues during neuronal development and in mature neurons by eliciting intracellular signaling through their endocytosis (13). This highlights the link between endocytosis and signaling as endosomes play a crucial role in signal transduction (14, 15). Furthermore, CAM depletion from the plasma membrane and subsequent degradation through the lysosomal pathway can change cell adhesion, a process important in the control of cell migration (16, 17). Understanding how CAR is linked to the intracellular machinery is also of particular importance for a better understanding of its endogenous function in the CNS as a role in neurite outgrowth was proposed (18), as well as in virus infection and gene transfer.

In this study, we characterized the mechanisms regulating CAR endocytosis and transport upon ligand binding in neurons. We found that CAR D1-D1 interaction disengagement, coupled to sequences in its cytoplasmic tail were responsible for ligand-induced CAR endocytosis. Moreover, we found that lipid microdomains, dynamin, and actin played crucial roles in CAR internalization. We also demonstrated that CAR was targeted to lysosomes for degradation in primary rodent neuron cultures and in the rodent brain.

EXPERIMENTAL PROCEDURES

Material, Constructs and Cellular Cultures—Labeled recombinant CTB (cholera toxin binding fragment), dextran and transferrin (Tf), as well as Alexa Fluor-conjugated secondary antibodies were purchased from Invitrogen. RmcB, a mouse monoclonal anti-CAR antibody was purchased from Millipore, the goat polyclonal anti-CAR antibody was from R&D Systems, and the rabbit polyclonal anti-CAR was generously provided by Joseph Zabner (University of Iowa). Polyclonal anti-flotillin-1 and monoclonal anti- β -tubulin were purchased from Sigma. Rat monoclonal anti-LAMP1 was purchased from Abcam. β 3-Tubulin (Tuj-1) antibody was purchased from Covance. Anti-Rab5 antibody was from Synaptic Systems. OptiPrepTM, filipin, Latrunculin A (LatA), methyl- β -cyclodextrin, E-64D, and pepstatin A were from Sigma.

Plasmids from the pcDNA-RFP-C backbone and encoding CAR-RFP and mutants 348, 315, and 261 were previously described (19). The pcDNA-CAR-274 construct was generated using site-directed mutagenesis. The AP2 ^{μ 2T156A} construct was a gift from E. Smythe and the dynamin^{K44A} construct was a gift from H. McMahon (Laboratory of Molecular Biology, Cambridge, UK).

Mouse hippocampal neurons were obtained from OF1 embryonic day 18 (E18) embryos using standard procedures.

Briefly, hippocampi were isolated, dissociated with 0.025% trypsin, and plated in Neurobasal medium (Invitrogen) containing B27 (Invitrogen), L-glutamine (Sigma), Glutamax (Invitrogen), 10% fetal bovine serum (FBS, Sigma), and antibiotics. Hippocampal neurons were then incubated at 37 °C and 5% CO₂ under a humidified environment. At day *in vitro* (DIV) 4, 2/3 of the medium was replaced with medium without L-glutamine and FBS. Neurons were used at DIV 10–14. Neu2A cells were cultured in DMEM (Invitrogen) containing 10% FBS and antibiotics.

siRNA Treatments—siRNAs against the murine clathrin heavy chain (CHC) were previously described (chc-1, 5'-AACAUUGGCUUCAGUACCUUGTT-3'; chc-2, 5'-AAUGGAUCUCUUUGAAUACGGTT-3) (20). Control siRNA was designed using the siRNA CHC-1 sequence and replacing 2 central nucleotides (control, 5'-AACAUUGGCAACAGUACCUUGTT-3'). siRNA duplexes were purchased from IDT Technologies and transfected in primary neurons according to a published method (21). Briefly, neurons at DIV 11 were co-transfected with a plasmid encoding GFP (pEGFP) and siRNA duplexes using Lipofectamine 2000. Three days later, ligands (FK^{CAV} or Tf) were applied and internalization was monitored. Knock-down of CHC was monitored using anti-clathrin antibody (clone X22) from Abcam.

Adenoviral Vectors and Recombinant Fiber Knob (FK^{CAV})—CAV-GFP, CAV-CRE, and HAdV5- β Gal were produced and purified using established methods (22, 23). To produce FK^{CAV} (residues 358–542), the cDNA was cloned into pPROEX HTb (Invitrogen), expressed with a cleavable His₆ tag, and purified as previously described (9). Labeled FK^{CAV} was obtained as previously described (8).

Flow Cytometry—Neu2A cells transfected with a plasmid encoding for CAR-RFP were collected in PBS (Invitrogen) and incubated for 1 h at 4 °C with anti-CAR RmcB. Cells were washed with PBS and incubated for 30 min with Alexa Fluor 488-labeled anti-mouse IgG antibody. As control, nontransfected cells incubated with anti-CAR and cells transfected and incubated with only the secondary antibody were used. Cells were washed with PBS, fixed with 2% paraformaldehyde, and analyzed with FACSCalibur (BD Biosciences). Compensation to avoid overlapping fluorescence between RFP and Alexa Fluor 488 was performed. Data analysis was performed using the FlowJo software.

Lipid Microdomain Isolation—Lipid microdomains were isolated with a modified protocol previously described (24). Briefly, cells were lysed using 250 mM sucrose, 1 mM MgCl₂, 1 mM CaCl₂, and 20 mM Tris-HCl, pH 7.5. The cellular homogenate was passed through a 25-gauge needle several times and centrifuged at 16,000 \times g for 10 min at 4 °C. The supernatant was put aside, the procedure repeated on the pellet, and the two supernatants pooled. Lipid microdomain fractions were obtained by ultracentrifugation in OptiPrepTM step density gradients. Two milliliters (ml) of the supernatant was mixed with an equal volume of 50% OptiPrep diluted in lysis buffer and transferred to a SW40 ultracentrifuge tube. 1.7 ml of 20, 15, 10, and 5% OptiPrep and lysis buffer (v/v) were successively overlaid. The tube was centrifuged at 75,000 \times g for 90 min at 4 °C. Fractions of 1 ml were removed from the top of the tube

Viral Ligands Induce CAR Endocytosis

and precipitated in 10% trichloroacetic acid overnight at 4 °C. Precipitates were then washed with cold acetone and solubilized in SDS-PAGE loading buffer.

Immunofluorescence and Confocal Microscopy—Hippocampal neurons plated on poly-D-ornithine coverslips or in microfluidic chambers (see below) were imaged using Leica LSM780 and Zeiss SP5 confocal microscopes, with $\times 63$ 1.4 NA Plan Achromat oil-immersion objectives.

For indirect immunofluorescence, neurons were fixed with 4% paraformaldehyde and permeabilized with 0.1% Triton X-100 for 5 min at room temperature (RT), followed by a blocking step with 2% bovine serum albumin (BSA) and 10% horse serum for 30 min to 1 h at RT. Primary and secondary antibodies were diluted in blocking solution and incubated sequentially for 1 h at RT. Samples were then mounted with fluorescent mounting medium (Dako) with DAPI (Sigma) and imaged by confocal microscopy.

Live cell imaging was performed as previously described (8). Briefly, 100–150 frames were acquired at 0.5 frames/s. Kymographs were generated using the Image J software.

Microfluidic Chambers—Microfluidic chambers (MCs) for neuronal compartmentalization were produced as previously described (25, 26). Briefly, polydimethylsiloxane inserts were covalently bound to glass bottom dishes (Wilco Dish) using a plasma cleaner (Deiner Electronic). MCs were then coated with 4% BSA for 2 h at 37 °C followed by poly-D-ornithine for 2 h at 37 °C. Devices were washed and further coated with laminin for 90 min at 37 °C. Dissociated neurons were plated in the proximal compartment and axonal growth through the microgrooves to the distal compartment was allowed for 5–8 days. To perform axonal transport experiments, distal compartments were fluidically isolated by using less volume than in proximal compartments.

Ethical Statement—The animals were treated in accordance with the European Community Council Directive 86/609, modified by the decrees 87/848 and 2001/464. The Animal Welfare Committee at the University of Montpellier 2 approved all protocols and all efforts were made to minimize the number of animals used and potential pain and distress. Pertinent license and permits (34-132) were obtained prior to institutional and regional animal welfare committee approval.

Intracerebral Injection of FK^{CAV}—6–7-Week-old female OF1 mice (Charles River) weighing 26–30 g were housed in groups prior to injections, and allowed food and water *ad libitum*. They were maintained in a controlled environment (22 ± 1 °C, $55 \pm 5\%$ humidity) with a 12 h:12 h light/dark cycle. Intrastriatal injections were performed in anesthetized animals with an intraperitoneal injection of a mixture of ketamine (80 mg/kg) and xylazine (10 mg/kg). To cover the entire striatum, we targeted four coordinates of injection according to a mouse brain atlas (80) (first and second sites of injection: anterior-posterior, +0.14 mm; lateral, +2 mm; dorsal-ventral, -3/-4 mm; third and fourth sites of injection: anterior-posterior, +1.10 mm; lateral, +1.5 mm; dorsal-ventral, -3/-3.75 mm). Animals were divided into several groups. One group received injections of PBS and a second group injections of FK^{CAV} (0.2, 1, or 5 μg /striatum). Each mouse was injected in one hemisphere; the contralateral striatum was used

as internal control. Mice were sacrificed by intracardiac fixation or decapitation 1, 7, 14, or 30 days post-injection. For the study of CAR expression by immunoblot, striata were dissected and proteins were extracted by sonication with 5% SDS. The location of the Cy5-tagged FK^{CAV} was evaluated in the striatum and the substantia nigra 1 day post-injection.

Statistical Analyses—Data were analyzed using Student's *t* test for unpaired data and one sample *t* test for data compared with control set as 100% (*, *p* value <0.05; **, *p* value <0.01; ***, *p* value <0.001 versus control). Results are expressed as mean \pm S.E.

RESULTS

Multiple Ligands Induced CAR Internalization in Primary Neurons and Neu2A Cells—Receptor engagement by viruses or viral proteins is often linked with conformational changes that can ultimately lead to endocytosis of the receptor-pathogen complex. To better understand the mechanism leading to CAR internalization, the role of ligand valency and CAR-CAR interactions, we incubated hippocampal neurons for 20 min at 37 °C after a pre-binding step on ice with multiple CAR ligands: FK^{CAV}, CAV-2, HAdV5, and anti-CAR antibodies (Fig. 1, A–E). Cultured hippocampal neurons from E18 express CAR at the membrane and possibly in intracellular compartments (data not shown), as we previously showed in primary motor neurons (8, 27). CAV-2 and FK^{CAV} led to CAR internalization in puncta that were also positive for Tf, which label endocytic structures (as observed in motor neurons (8)) (Fig. 1, A, B, and E). We also detected internalized CAR after incubation with HAdV5, suggesting that other CAR-tropic AdVs also triggered CAR internalization (Fig. 1, C and E). One possible explanation for ligand-induced CAR internalization was that its clustering through multivalent interactors initiate subsequent endocytosis. To test whether clustering *per se* was responsible for CAR entry, we used anti-CAR antibodies recognizing epitopes on the extracellular domains of CAR (see “Experimental Procedures”). In contrast to trivalent (FK^{CAV}) or multivalent (AdV) ligands, anti-CAR antibodies did not lead to CAR internalization in hippocampal neurons (Fig. 1, D and E), suggesting that clustering of CAR through multimeric ligands was not sufficient for its internalization. Notably, recombinant FKs and AdVs can disrupt CAR D1-D1 interactions (28).

This differential ligand-induced internalization was also seen in CAR-transfected Neu2A cells, a mouse line derived from a murine neuroblastoma with undetectable CAR expression (Fig. 2A). In Neu2A cells transfected with a plasmid expressing CAR-RFP and then incubated with FK^{CAV}, CAV-2, or HAdV5, the ligands were found in vesicular structures together with CAR, similarly to hippocampal neurons. Notably, cells incubated with anti-CAR antibodies did not contain intracellular puncta of CAR (Fig. 2, B and C). To test these observations using another method, we monitored CAR plasma membrane levels using flow cytometry. Neu2A cells were transfected with a plasmid encoding CAR-RFP, and then incubated overnight with FK^{CAV}, CAV-2, or HAdV5. In these conditions, we found a decrease in plasma membrane CAR (Fig. 2D), and therefore conclude that viral ligands triggered CAR internalization. Of note, at similar physical particle per cell ratio (pp/c), CAV-2

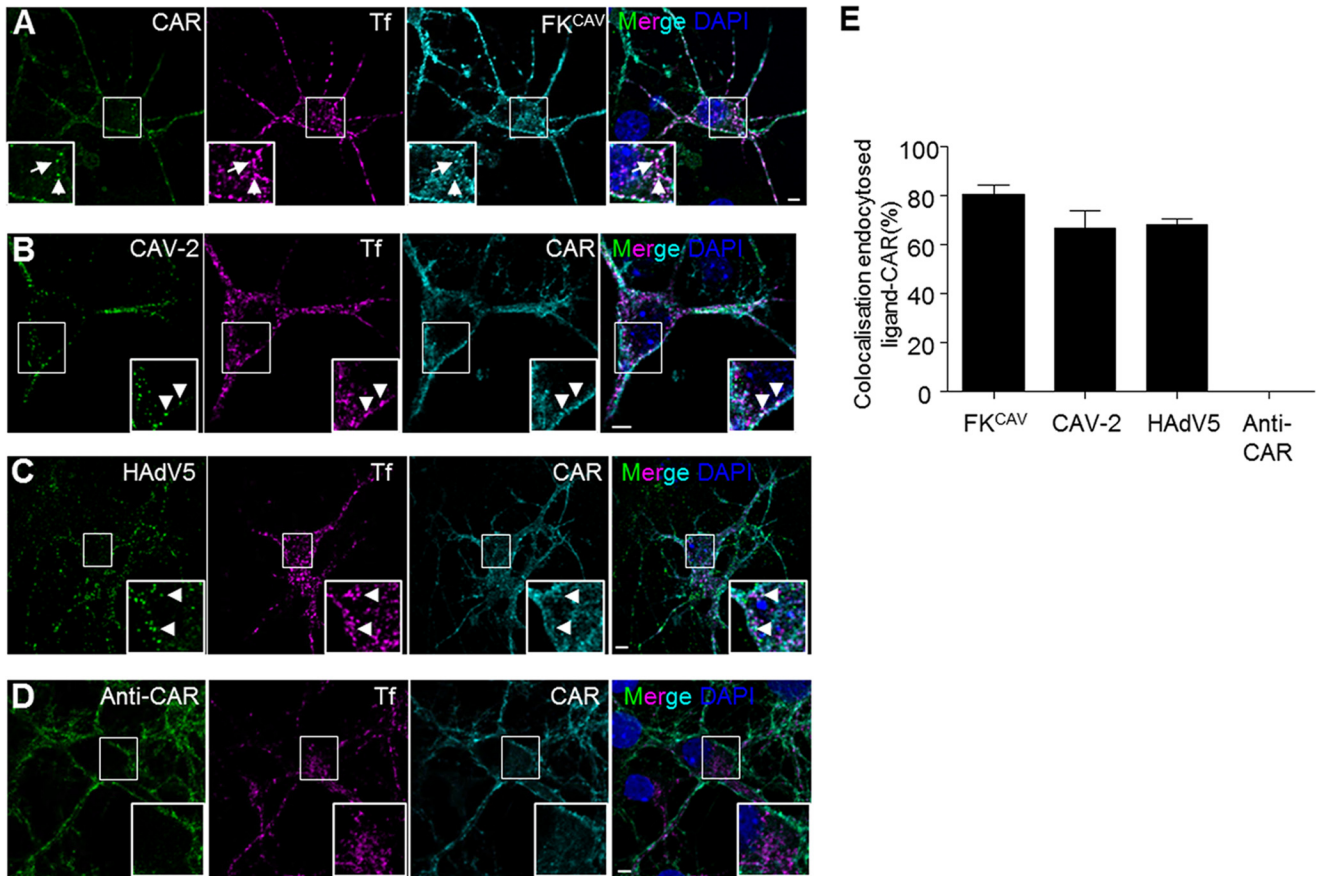


FIGURE 1. CAR was endocytosed after viral ligand binding in hippocampal neurons. A–D, viral ligands induced CAR internalization. Hippocampal neurons were incubated with FK^{CAV} (0.6 μ g/ml) (A), CAV-2 (2,000 pp/c) (B), HAdV5 (2,000 pp/c) (C), or anti-extracellular CAR (D) together with Alexa 555-Tf for 15 min on ice, and washed, and internalization was allowed for 20 min at 37 °C. Fixed cells were labeled for endogenous CAR. CAR can be found in endocytic vesicles positive for Tf (indicated by *arrows*) after FK^{CAV}, CAV-2, and HAdV5 engagement, but not after anti-CAR binding. E, quantification of three independent experiments shows that internalized ligands (co-localizing with Tf) are found with CAR ($n = 3$, ≥ 107 vesicles counted for each condition; results are expressed as mean \pm S.E.). Scale bars: A–D, 5 μ m.

induced CAR internalization more efficiently than HAdV5 (Fig. 2D). Together, these data showed that CAR can be internalized in neuronal cells, but different efficacies in ligand-dependent internalization existed.

CAR Is Located within Lipid Microdomains at the Plasma Membrane and during Internalization in Neurons—The plasma membrane is organized in subdomains where proteins and lipids can elicit specific signals, regulate cell adhesion, and other processes. Among these domains, lipid microdomains have unique properties that diversify membrane trafficking and signaling (29). Because numerous viral and toxin receptors, including CAR (30, 31), are located within lipid microdomains, we assayed the membrane sublocalization of CAR in primary neuron cultures and in the mouse brain. When using a detergent-free method (24) to isolate lipid microdomains from primary cortical neurons, flotillin-1, a marker for lipid microdomains, was found in the top fractions of the density gradient (Fig. 3A). CAR was mainly found in flotillin-1⁺ fractions, suggesting that CAR was a resident of lipid microdomains in neurons (Fig. 3A). To monitor the dynamic association of CAR with lipid microdomains, we used methyl- β -cyclodextrin to remove cholesterol from membranes and shift lipid microdomain-associated proteins toward the bottom of the density gradient.

Under these conditions, CAR and flotillin-1 were found in the bottom fractions of gradient of cortical neurons (Fig. 3A).

AdVs use multiple receptors to engage and enter cells. The paradigm is that CAR-bound AdVs are internalized via interaction with integrins through an RGD motif in the penton base (32). To circumvent the role of co-receptors, which could bias the interpretation of CAR membrane dynamics, we used FK^{CAV} as a CAR-specific ligand. We previously showed that when motor neurons were incubated with a mutant form of FK^{CAV}, FK^{CAV} Δ CAR, where the CAR-binding site was ablated, we could not detect CAR interaction via surface plasma resonance, cell binding, or CAR endocytosis (8, 9). These data were consistent with the specificity of FK^{CAV} to detect CAR.

Some proteins, such as the epidermal growth factor receptor (EGFR), can diffuse laterally out of lipid microdomains during clathrin-dependent internalization (33). To test whether CAR would also leave these microdomains during binding or the first steps of entry, we assayed its lipid microdomain location after ligand engagement. FK^{CAV} was incubated with cells at 4 °C to allow attachment, and then \pm 20 min at 37 °C to allow internalization. Using this assay, we found that CAR did not exit lipid microdomains after FK^{CAV} binding or internalization (Fig. 3B). Similarly, neither CAV-2 nor HAdV5 displaced CAR from

Viral Ligands Induce CAR Endocytosis

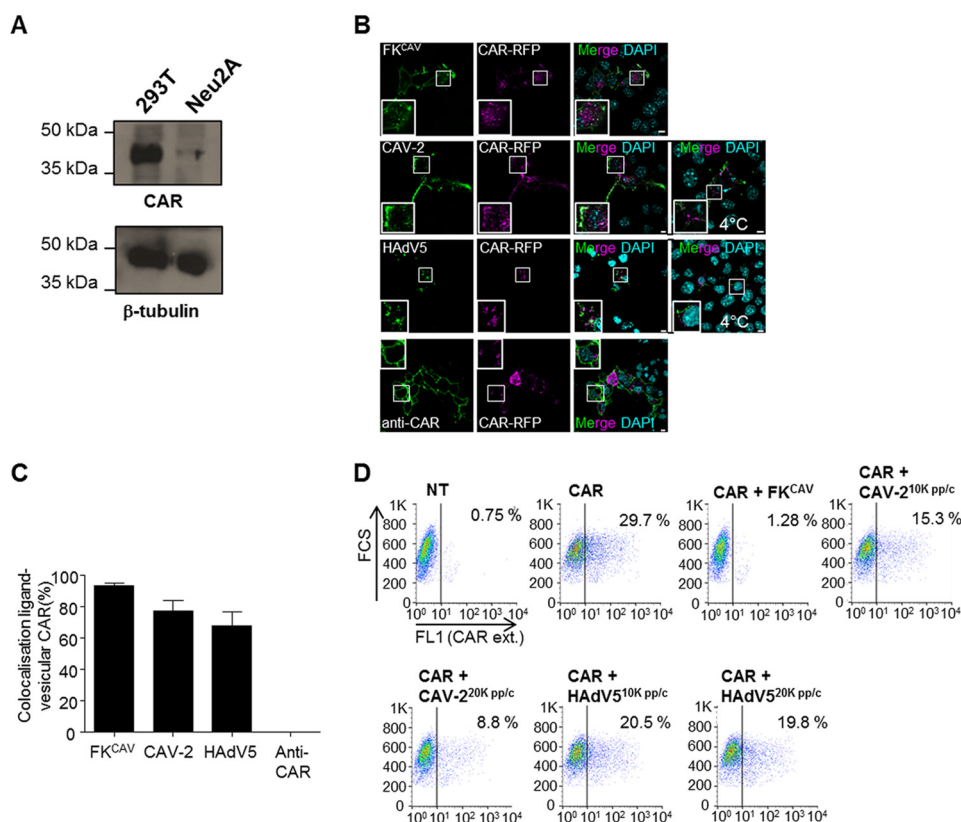


FIGURE 2. CAR was endocytosed after viral ligand binding in Neu2A cells. *A*, Neu2A cells did not express CAR. Western blot analyses showed that in contrast to 293T cells, Neu2A did not express detectable levels of CAR. *B*, viral ligands triggered CAR-RFP internalization in Neu2A cells. Cells were transfected with a plasmid encoding for CAR-RFP and 24 h later, incubated with FK^{CAV}, CAV-2 (2,000 pp/c), HAdV5 (2,000 pp/c), or anti-extracellular CAR on ice for 20 min and placed at 37 °C for 30 min. Only viral ligands triggered CAR relocation in vesicular structures (*insets* show colocalization of CAR and viral ligands compared with CAV-2 and HAdV5 incubation only on ice or anti-CAR applied live). *C*, quantification of three independent experiments showed that ligands were found with vesicular CAR ($n = 3$, ≥ 93 vesicles counted for each condition; results are expressed as mean \pm S.E.). *D*, flow cytometry analyses showed a decrease of plasma membrane CAR after viral ligand engagement. Neu2A cells were transfected or not with a plasmid encoding for CAR for 24 h, incubated on ice for 20 min with either 1 μ g of FK^{CAV}, 10,000 or 20,000 pp/c of CAV-2, or 10,000 or 20,000 pp/c of HAdV5, and shifted to 37 °C overnight. Cells were scrapped in PBS and labeled for external CAR (CAR ext.) according to "Experimental Procedures." Scale bars: *A*, 10 μ m; *C*, 5 μ m.

these microdomains (Fig. 3*B*). We then asked whether lipid microdomain integrity was needed for CAR internalization. We incubated hippocampal neurons with filipin, a lipid microdomain-disruptor, prior to FK^{CAV} binding. In this condition, the internalization of FK^{CAV}/CAR and the binding domain of CTB, which recognizes the ganglioside GM1, a well characterized lipid microdomain component, was prevented. By contrast, Tf internalization, which uses a non-lipid microdomain entry pathway, was not (Fig. 3, *C* and *D*). This suggested that the main route of entry of CAR in neurons required the integrity of lipid microdomains.

Together, these data demonstrated that CAR was a permanent resident of lipid microdomains in neurons in native conditions, and during ligand-induced internalization. Furthermore, the association of CAR with lipid microdomains was crucial in its ability to undergo endocytosis as sequestration of cholesterol blocked its internalization.

Clathrin-independent, Dynamin- and Actin-dependent CAR Endocytosis in Neurons—Lipid microdomain-dependent and clathrin-dependent endocytosis were, until recently, thought to be largely independent. This is illustrated by the data concerning EGF/EGFR endocytosis, which can happen in lipid microdomains, or after lateral diffusion outside them, and then engaging the clathrin machinery (33). However, this view has

been tempered by reports suggesting that clathrin-dependent endocytosis could take place into lipid microdomains (34). In epithelial cells, numerous studies showed that AdV entry involves the clathrin machinery (35). Notably, the intracellular domain of CAR has a functional tyrosine-based AP (adaptor protein) binding site YXX ϕ (YNQV; Fig. 4*A*) that is present in numerous receptors that use clathrin machinery for endocytosis. This motif was reported to be involved in the basolateral sorting of CAR through AP1 in epithelial cells (36). However, the role of YNQV as an internalization sequence has not been characterized for CAR. We therefore used transfected Neu2A cells with plasmids encoding CAR-RFP deletion mutants lacking the PDZ (PSD-95/Discs-large/ZO-1) binding domain and the potential AP binding site (Fig. 4, *A* and *B*). When we incubated FK^{CAV} with cells expressing the full-length (FL) CAR-RFP at 4 °C, we found FK^{CAV} bound only on transfected cells, showing the specificity for plasma membrane CAR (data not shown). We then shifted cells to 37 °C to monitor CAR endocytosis. Under these conditions, FK^{CAV} and CAR were co-internalized in endocytic vesicles (Fig. 4, *C* and *D*). Neu2A cells expressing CAR-RFP with a deletion in the AP binding site (CAR-315) also bound FK^{CAV} at 4 °C. After inducing internalization at 37 °C, endocytosis was similar to full-length CAR (Fig.

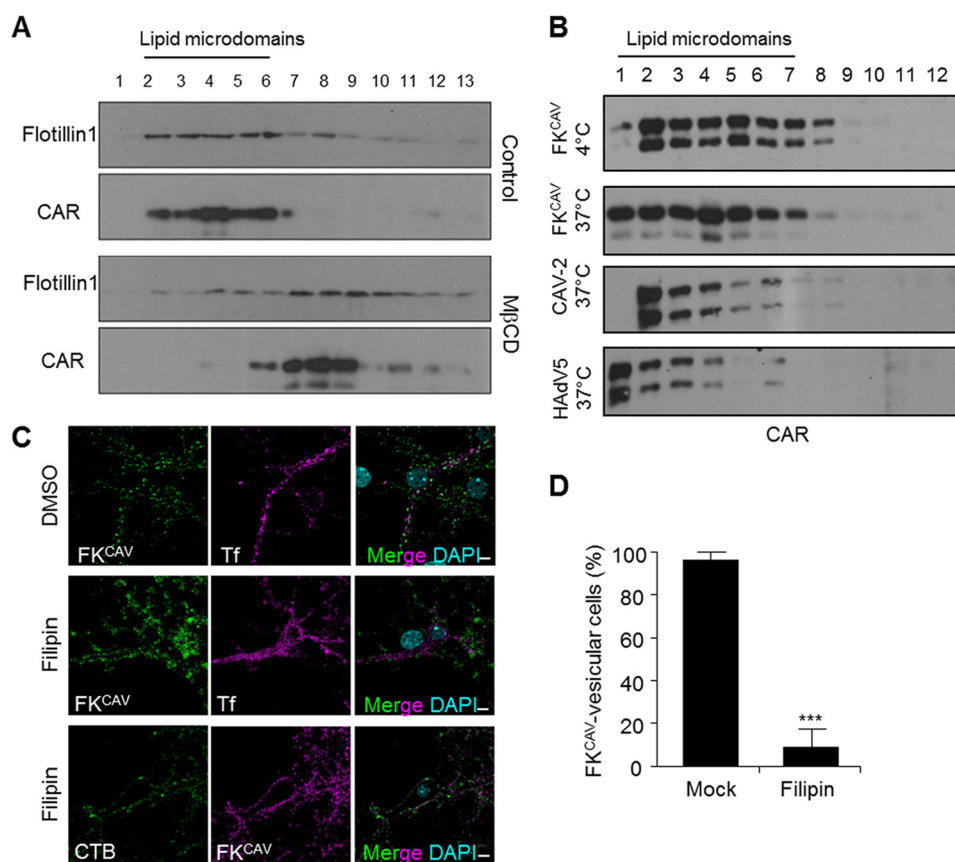


FIGURE 3. CAR location in lipid microdomains at the plasma membrane and during internalization. *A*, CAR was found in flotillin-1⁺ fractions, a lipid microdomain protein in mouse cortical neuron extract subjected to biochemical isolation through OptiPrep gradient. Cortical neurons were incubated with 10 mM methyl- β -cyclodextrin (*MβCD*), a known lipid microdomain destabilizer, and subjected to lipid microdomain isolation. Methyl- β -cyclodextrin triggered flotillin-1 and CAR relocation in lower fractions. Western blots are representatives of 3 independent experiments. *B*, CAR did not exit lipid microdomains after ligand binding and internalization. Lipid microdomain isolation was performed on cortical neurons incubated either with FK^{CAV} on ice, or shifted to 37 °C for 20 min after incubation on ice with FK^{CAV}, 10,000 pp/c CAV-2, or 10,000 pp/c HAdV5. Western blots are representatives of three independent experiments. *C*, filipin blocked CAR internalization. Hippocampal neurons were treated with 5 μ g/ml of filipin for 30 min prior to FK^{CAV}/Tf or FK^{CAV}/CTB incubation on ice for 20 min. Cells were washed and then shifted to 37 °C for 1 h to trigger internalization. In contrast to Tf, CTB and FK^{CAV} did not enter after filipin treatment. *D*, quantification of three independent experiments showed that filipin efficiently blocked FK^{CAV} internalization ($n = 3$, ≥ 45 cells counted for each condition; results are expressed as mean \pm S.E. ***, p value < 0.001 versus control). Scale bar, 5 μ m.

4, *C* and *D*), suggesting that clathrin-dependent endocytosis was unlikely to be the major route of internalization of CAR.

To identify the sequence involved in CAR internalization, we carried out a more extensive deletion analyses. We found that the sequence necessary for FK^{CAV}-mediated endocytosis of CAR was between amino acids 261 and 274, as CAR-274 was internalized but CAR-261 was not (Fig. 4, *C* and *D*). To test if this conclusion held true in primary neurons, CAR-RFP plasmids were transfected in hippocampal neurons that were subsequently incubated with FK^{CAV}. Similarly to that found in Neu2A, CAR-261 failed to internalize FK^{CAV} (Fig. 4, *E* and *F*).

To address the role of clathrin-mediated endocytosis using another approach, we transfected Neu2A cells and hippocampal neurons with a plasmid expressing AP2 μ 2^{T156A}, a dominant-negative construct that blocks clathrin-dependent endocytosis (37). AP2 μ 2^{T156A} inhibited Tf uptake, which is dependent on the clathrin machinery (Fig. 5*A*). However, in Neu2A (Fig. 5, *A* and *B*) and hippocampal neurons (Fig. 5, *C* and *D*) expressing AP2 μ 2^{T156A} and CAR-GFP, FK^{CAV} was efficiently internalized. Similarly, hippocampal neurons co-transfected with a plasmid harboring a GFP expression cassette to identify transfected cells and two different siRNAs against the

CHC was not blocking FK^{CAV} internalization, which supports our conclusion that CAR did not use the clathrin machinery for its internalization upon FK^{CAV} engagement (Fig. 5, *E* and *F*). Similar results were obtained in Neu2A cells transfected with CAR-GFP (data not shown). We then assayed the role of dynamin, a GTPase involved in the fission of clathrin-coated vesicles, and also in lipid microdomain-mediated pathways (38). We transfected plasmids expressing the dominant-negative construct dynamin2^{K44A} (Dyn2^{K44A}) that cannot hydrolyze GTP and therefore inhibits dynamin-mediated membrane fission (39). Expression of Dyn2^{K44A} strongly decreased Tf and CAR internalization in Neu2A cells co-transfected with CAR-GFP, and in hippocampal neurons (Fig. 5, *A–D*), suggesting that dynamin was involved in CAR endocytosis after FK^{CAV} engagement.

As actin filaments are involved in the endocytosis of numerous receptors (40), we then assayed the role of actin in CAR internalization. Huang *et al.* (41) previously showed that CAR interacts with actin, suggesting that the actin cytoskeleton could play a role in its trafficking. To monitor the role of actin, we used LatA, which induces the disassembly of actin polymers. We transfected Neu2A cells with CAR-GFP, incubated them at

Viral Ligands Induce CAR Endocytosis

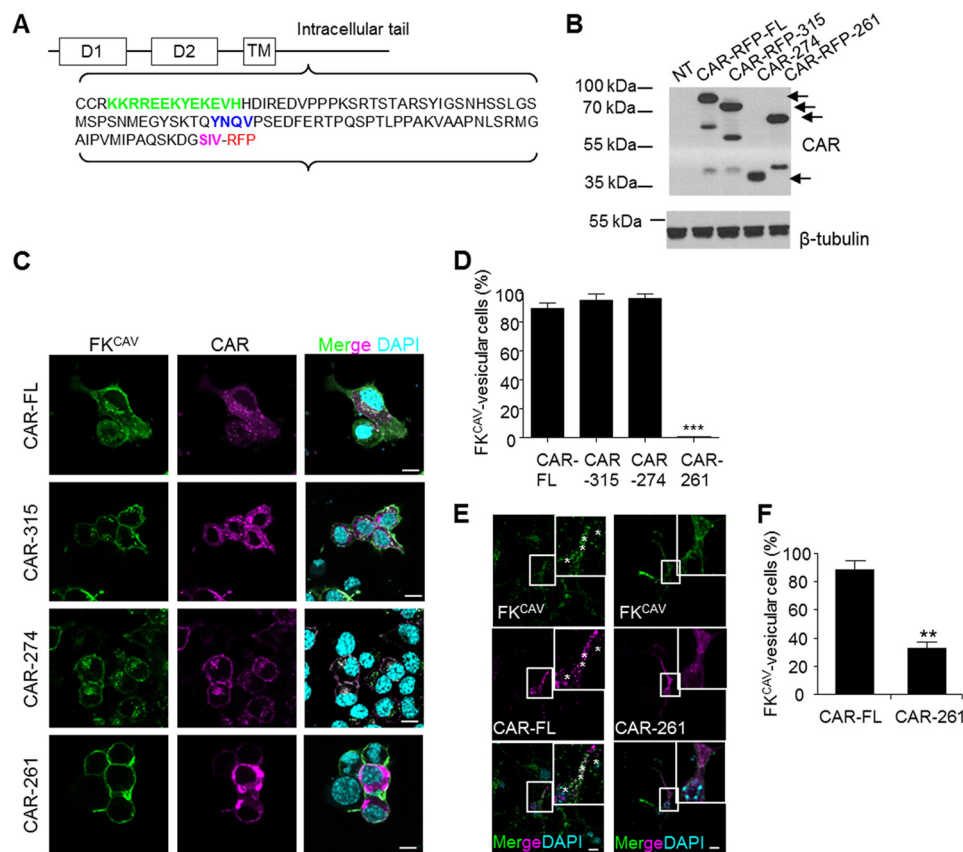


FIGURE 4. Cytoplasmic sequence necessary for CAR internalization. *A*, CAR intracellular domain sequence. AP binding site is highlighted in blue, PDZ-binding domain in magenta, and minimum sequence needed for internalization in green. *B*, expression of CAR constructs in Neu2A cells. Cells were transfected, collected 24 h later and total extracts subjected to SDS-PAGE analyses using an anti-CAR raised against the extracellular domain. *C*, the AP binding site is not necessary for CAR internalization. Neu2A cells were transfected with CAR-RFP or its mutants. 24 h later, FK^{CAV} was added for 20 min on ice, the medium was replaced and internalization was allowed for 1 h at 37 °C. Cells were fixed and stained using an antibody anti-FK. Only the construct CAR-261 did not allow FK^{CAV} internalization. *D*, quantification of FK^{CAV} internalized cells ($n =$ three independent experiments, ≥ 50 cells counted for each condition; results are expressed as mean \pm S.E. ***, p value < 0.001 versus control). *E*, hippocampal neurons were transfected with CAR-RFP or CAR-261 and similar procedures were applied. As above, CAR-261 did not internalize FK^{CAV}. *Insets* show CAR-FL and FK^{CAV} in vesicular structures (asterisks), whereas in CAR-261-transfected cells, FK^{CAV} was mainly at the plasma membrane. *F*, quantification of FK^{CAV}-internalized cells ($n = 3$ independent experiments, ≥ 21 cells counted for each condition; results are expressed as mean \pm S.E. **, p value < 0.01 versus control). Scale bars, 10 μ m.

4 °C with FK^{CAV} and then shifted them at 37 °C for 1 h. In these conditions, cells pre-treated with LatA failed to internalize FK^{CAV}, whereas in DMSO-treated cells FK^{CAV} was found in endosomes (Fig. 6, *A* and *B*). Similarly, in mock-treated cells FK^{CAV} was present in endosomes 1 h post-internalization, whereas LatA treatment maintained a membrane-bound pattern of FK^{CAV} in hippocampal neurons, consistent with an inhibition of internalization (Fig. 6, *C* and *D*).

Taken together, these data suggested that in neurons, CAR was linked to a lipid microdomain-, actin-, and dynamin-dependent route of internalization. In addition, the AP binding site in the intracellular tail of CAR was not necessary for its endocytosis, consistent with its uptake via a clathrin-independent route.

FK^{CAV}-induced CAR Internalization in Neurons Is Coupled to the Endolysosomal Pathway—Receptor function can be modulated by the preferential targeting to subcellular compartments upon ligand-induced internalization. After endocytosis, ligand-receptor complexes can be recycled back to the plasma membrane, targeted to the *trans*-Golgi network and endoplasmic reticulum, or degraded by lysosomes. During their endocytosis, AdVs trigger endosomal lysis to reach the cytosol. This

phenomenon precludes the identification of the trafficking of CAR after endocytosis. We therefore used FK^{CAV} to induce CAR internalization and characterized its trafficking post-entry. When hippocampal neurons were incubated with FK^{CAV}, we detected a relocalization of endogenous CAR that led to its disappearance from neurites and its accumulation in the cell body (data not shown). This could be interpreted in at least two ways: active transport (as previously shown) or distal degradation. To determine whether CAR entered the recycling pathway, we co-incubated hippocampal neurons with FK^{CAV} and Tf on ice, then shifted the neurons to 37 °C for various times. Tf and its receptor TfR are markers of the recycling pathway and reach early endosomes prior to targeting recycling endosomes and the plasma membrane. FK^{CAV} and Tf colocalized at the early time point but then separated, suggesting that CAR was not targeted to recycling endosomes (Fig. 7, *A* and *B*).

As CTB uses a lipid microdomain-dependent endocytic pathway (42), which transports the toxin from endosomes to the Golgi apparatus, we monitored the possible co-transport of CAR within this route. To this end, we co-incubated hippocampal neurons with FK^{CAV} and CTB as above. Although FK^{CAV}/CAR colocalized with CTB at early time points and was in peri-

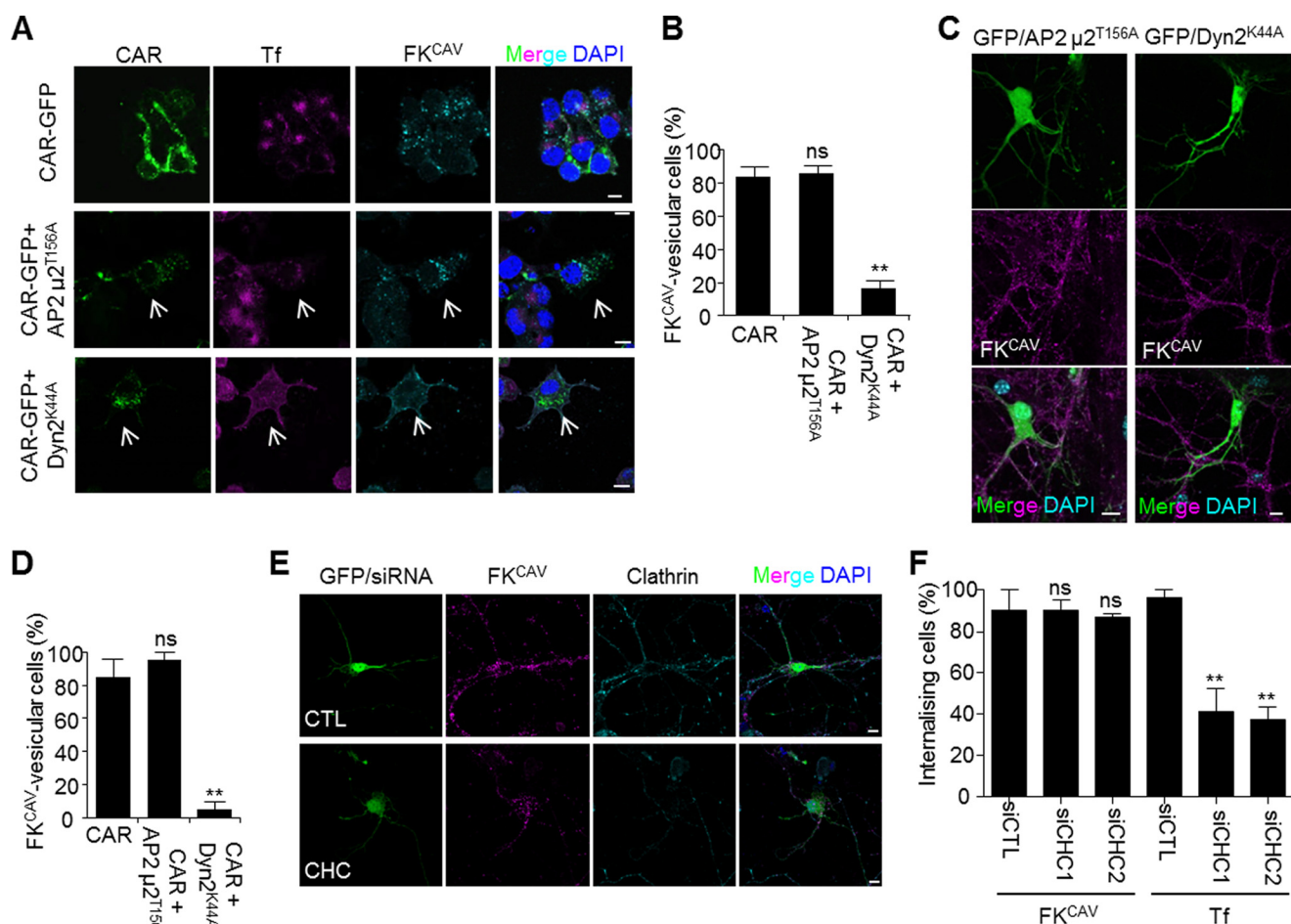


FIGURE 5. Clathrin-independent and dynamin-dependent CAR internalization. *A* and *B*, dynamin mutant blocked CAR internalization in Neu2A cells, whereas inhibition of the clathrin-mediated entry did not have an effect. Neu2A cells were transfected with CAR-GFP alone, or in combination with plasmids encoding AP2 μ 2^{T156A} or dynamin2^{K44A} and 24 h later incubated with FK^{CAV} on ice for 20 min, rinsed, and internalization was allowed for 1 h at 37 °C. Cells were fixed and the FK^{CAV}/CAR location was analyzed by confocal microscopy. *Arrows* show cells expressing dominant-negative mutants where Tf internalization was inhibited. FK^{CAV} was not internalized in cells expressing Dynamin2^{K44A}. *B*, quantification showed that inhibition of clathrin entry had no effect on FK^{CAV}/CAR internalization, whereas the dynamin mutant significantly decreased FK^{CAV}/CAR vesicular pattern ($n =$ three independent experiments, ≥ 58 cells counted for each condition; results are expressed as mean \pm S.E. **, p value < 0.01 versus control). *C*, hippocampal neurons were co-transfected with pEGFP and plasmids encoding AP2 μ 2^{T156A} or dynamin2^{K44A}, and FK^{CAV}/CAR internalization was observed using similar methods than with Neu2A cells. Dynamin inhibition showed similar blockade in the uptake of FK^{CAV}/CAR, whereas inhibition of clathrin-mediated endocytosis did not show a detectable effect. *D*, quantification of three independent experiments (≥ 19 cells counted for each condition; results are expressed as mean \pm S.E. **, p value < 0.01 versus control). *E*, hippocampal neurons were co-transfected with pEGFP and siRNAs against CHC or control siRNA. Three days post-transfection FK^{CAV} or Tf were applied and allowed to internalize for 90 min. CHC was visualized by indirect immunofluorescence to monitor knock-down. *F*, quantification of FK^{CAV} and Tf-internalized cells ($n =$ three independent experiments, ≥ 20 cells counted for each condition; results are expressed as mean \pm S.E. **, p value < 0.01 versus control). Scale bars, 10 μ m.

nuclear organelles at late time points, they did not colocalize with CTB at the *trans*-Golgi network (Fig. 7, *C* and *D*), as seen by three-dimensional rendering (Fig. 7*E*).

We repeated the above assay and stained FK^{CAV}-incubated neurons with LAMP1, a lysosomal marker. At 2 h post-internalization, numerous organelles were FK^{CAV}/LAMP1⁺ (Fig. 7*F*). To control for targeting of FK^{CAV} to lysosomes, we assayed the colocalization of FK^{CAV} and endogenous CAR 2 h post-internalization by immunofluorescence (data not shown). Similarly, when we incubated hippocampal neurons with FK^{CAV} overnight, we detected an $\sim 60\%$ decrease in CAR levels by immunoblot analyses, consistent with ligand-induced degradation (Fig. 7, *G* and *H*). CAR degradation was almost completely blocked by pre-treating cells with pepstatin A/E-64d or chloroquine, drugs that perturb lysosomal function (Fig. 7, *G* and *H*). Incubating cells with an anti-CAR antibody did not lead to its degradation, consistent with the immunofluorescence data

regarding its internalization (Fig. 7, *G* and *H*). From these data, we concluded that the primary fate of CAR after ligand-induced internalization was toward lysosomal degradation, and not the retrograde or recycling pathways.

Lipid Microdomain- and Actin-dependent Axonal-specific CAR Endocytosis and Somatodendritic Lysosomal Targeting—The composition of neuronal subcompartments such as dendrites and axons can differ greatly and possibly influence ligand-receptor endocytosis. To better understand ligand uptake at different neuronal sites, we used MCs (43). Hippocampal neurons were cultured for 5–8 days to allow axons to cross the microgrooves. Incubation in the axonal compartment with FK^{CAV} led to efficient retrograde transport of FK^{CAV} and accumulation of CAR in cell bodies (data not shown). As observed in batch cultures, $\sim 75\%$ of the CAR⁺ retrograde carriers were also CTB⁺ when the axonal compartment was co-incubated with FK^{CAV} and CTB, suggesting that lipid microdo-

Viral Ligands Induce CAR Endocytosis

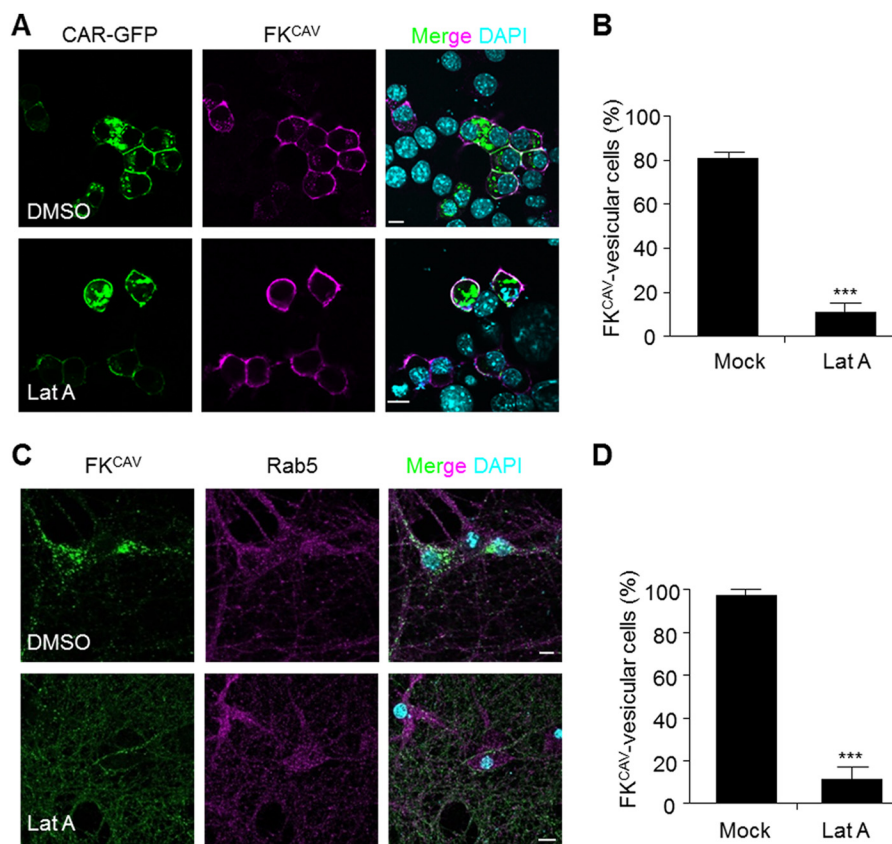


FIGURE 6. Actin dynamic regulation of CAR internalization. *A–D*, inhibition of actin disassembly blocked CAR internalization. *A*, Neu2A cells transfected with a plasmid encoding for CAR-GFP and pre-treated 24 h later with LatA ($10\ \mu\text{M}$) for 2 h at $37\ ^\circ\text{C}$ and further incubated for 1 h at $37\ ^\circ\text{C}$ with FK^{CAV} . *B*, quantification show that perturbation of actin dynamics blocked FK-induced internalization of CAR ($n =$ three independent experiments, ≥ 105 cells counted for each condition; results are expressed as mean \pm S.E. ***, p value < 0.001 versus control). *C*, hippocampal neurons were pre-treated with LatA ($10\ \mu\text{M}$) for 2 h at $37\ ^\circ\text{C}$ and further incubated for 1 h at $37\ ^\circ\text{C}$ with FK^{CAV} . *D*, quantification to show efficient impairment of FK^{CAV} internalization by LatA ($n =$ three independent experiments, ≥ 26 cells counted for each condition; results are expressed as mean \pm S.E. ***, p value < 0.001 versus control). Scale bars, $10\ \mu\text{m}$.

main-rich structures mediated the axonal retrograde transport of CAR (Fig. 8, *A* and *B*). However, after axonal transport, FK^{CAV} and CTB did not colocalize in the *trans*-Golgi network (Fig. 8*C*), whereas retrograde FK^{CAV} was found in LAMP1^+ somatodendritic structures (Fig. 8*D*). These data suggest a sorting mechanism once axonal cargoes reached the cell body and that CAR was targeted to lysosomes after retrograde transport.

To monitor whether the endocytic pathway regulating axonal entry and transport was similar to that in batch cultures, we assayed the effect of lipid microdomain disruption on FK^{CAV} /CAR axonal transport. When axon termini were preincubated with filipin, FK^{CAV} and CTB failed to accumulate in the soma, whereas rhodamine/dextran, a fluid phase marker, did (Fig. 9, *A* and *B*). Similarly, when axons were treated with LatA prior to FK^{CAV} incubation, we did not detect efficient FK^{CAV} accumulation in cell bodies after axonal transport (Fig. 9, *C* and *D*).

Together, these data showed that axonal endocytic trafficking of CAR was coupled to lipid microdomain- and actin-mediated endocytosis. In addition, retrograde co-transport with other lipid microdomain-dependent ligands was followed by a sorting to different somatodendritic destinations.

Ligand-induced CAR Axonal Transport and Degradation Occur *in Vivo*—Finally, we asked whether CAR trafficking and degradation occurred in the mammalian brain. To address this,

we injected FK^{CAV} in the striatum of 8-week-old mice. Using immunofluorescence, we found that FK^{CAV} was efficiently retrogradely transported from the striatum to the cortex and *substantia nigra* (SN) (Fig. 10*A*). This retrograde transport was also observed in the sciatic nerve after intramuscular injections (8). Eighteen hours post-injection, ipsilateral and contralateral striata were removed and proteins extracted. An $\sim 80\%$ decrease in CAR levels in FK^{CAV} -injected striata was detected compared with the contralateral structure, whereas mock (PBS) did not induce this phenomenon (Fig. 10*B*). Ligand-induced CAR degradation was dose-dependent (Fig. 10*B*) and CAR levels started to return to normal around 1 month post-injection (Fig. 10, *C* and *D*). Together, these data showed that after internalization, CAR was targeted to lysosomes for degradation *in vivo*.

DISCUSSION

In this study, we defined the mechanisms regulating CAR endocytic trafficking upon ligand binding. We showed that CAR-tropic AdVs and adenoviral proteins induced CAR internalization in neurons and neuronal cells. Endocytosis was lipid microdomain-, actin-, and dynamin-dependent, and did not require clathrin and its adaptors. Somatodendritic and axonal endocytosis targeted CAR to lysosomes leading to its degradation. Although CAR and CTB/GM1 shared common a lipid-microdomain entry/transport pathway, they differed in terms

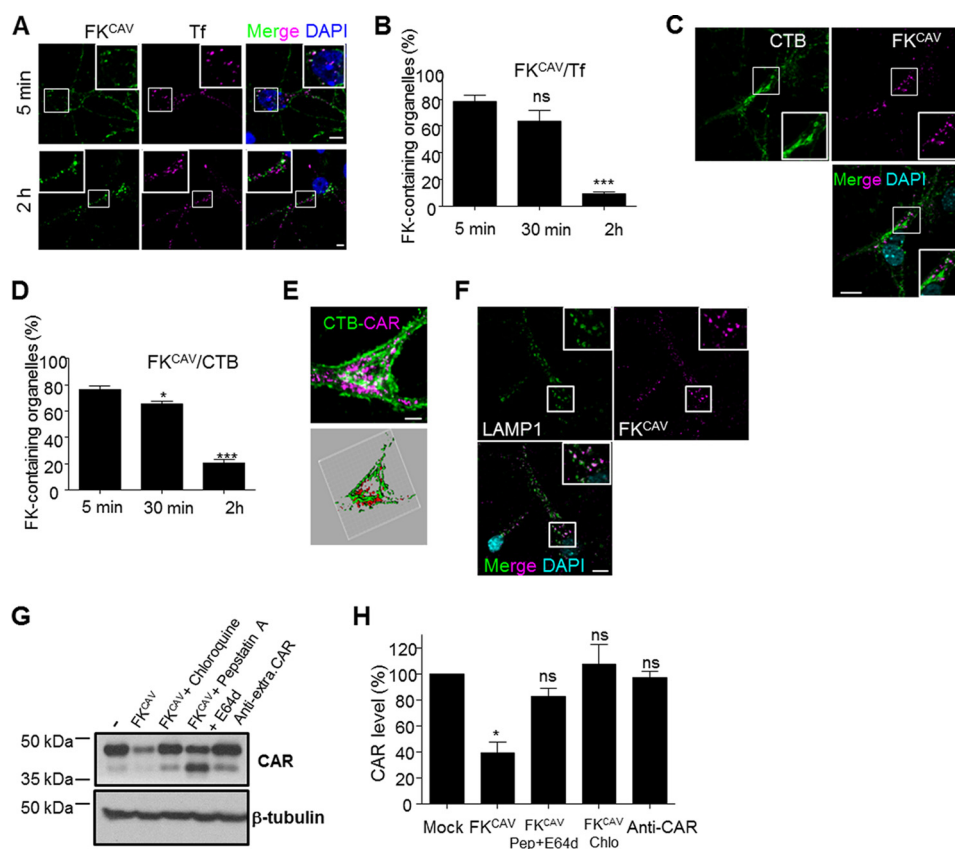


FIGURE 7. CAR was not linked to recycling or retrograde pathways, but was targeted to lysosomes. *A* and *B*, FK^{CAV} /CAR did not accumulate in recycling endosomes after internalization. *A*, hippocampal neurons were incubated with FK^{CAV} and Alexa 555-Tf on ice, the ligands were washed out, and the cells were placed at 37 °C for various times. Representative images of early (5 min) and late (2 h) endocytosis of FK^{CAV} and Alexa 555-Tf. *Insets* show colocalization early between FK^{CAV} and Tf but not at later points. *B*, quantitative analyses of three independent experiments showed significant loss of colocalization of FK^{CAV} and Alexa 555-Tf during progression of endocytosis ($n = 3$, ≥ 140 structures were counted for each time point; results are expressed as mean \pm S.E. ***, p value < 0.001 versus control). *C–E*, FK^{CAV} /CAR did not accumulate in the *trans*-Golgi network after internalization. *C*, representative images of late (2 h) endocytosis of FK^{CAV} and Alexa 488-CTB. *D*, quantitative analyses of three independent experiments showed loss of colocalization of FK^{CAV} and Alexa 488-CTB during progression of endocytosis ($n = 3$, ≥ 190 structures were counted for each time point; results are expressed as mean \pm S.E. *, p value < 0.05 ; ***, p value < 0.001 versus control). *E*, three-dimensional reconstruction shows a separation between FK^{CAV} and CTB. *F*, CAR was targeted to lysosomes after internalization. Hippocampal neurons were incubated with FK^{CAV} for 2 h and stained for lysosomes (LAMP1). *Insets* show strong colocalization ($87.7 \pm 3.5\%$; $n =$ three independent experiments, 315 structures were counted. Results are expressed as mean \pm S.E.). *G*, biochemical analyses of hippocampal neurons incubated overnight with FK^{CAV} \pm lysosomal chloroquine and pepstatin A + E-64d showed CAR degradation. Anti-CAR antibodies did not trigger CAR lysosomal hydrolysis. *H*, quantification of CAR lysosomal degradation ($n =$ three independent experiments, results are expressed as mean \pm S.E. *, p value < 0.05 versus control set as 100%). *Scale bars*: *A* and *D*, 5 μm . *C* and *F*, 10 μm .

of their final destination after axonal retrograde transport, suggesting a sorting mechanism at the soma-axon interface.

Numerous pathogens use plasma membrane receptors to access and spread in the CNS (1, 4). For instance, herpes simplex virus 1 (HSV-1) interacts with nectin-1, a CAM located at sensory terminals (44). Similarly, in motor neurons poliovirus binds CD155 to be endocytosed and retrogradely transported through direct interaction of the receptor with cytoplasmic dynein (45). As viral diseases can lead to severe pathologies such as paralysis or dementia, numerous efforts have been made to better characterize the host-pathogen interaction and the endogenous function of their cellular receptor(s).

Although AdVs are not quintessential human brain pathogens, they can be associated with encephalitis and brain tumors in humans and other species (46–50). Moreover, some AdV vectors are particularly promising for gene transfer to the CNS (51, 52). For instance, vectors derived from CAV-2 preferentially transduce neurons and their efficient axonal retrograde transport allows a widespread transduction in the CNS of

rodents and dogs (27, 53). To better understand CAV-2 tropism and transport, we previously analyzed its axonal transport in motor neurons (8). We showed that CAV-2 transport from nerve termini to the cell body was in pH-neutral vesicles, which underwent a maturation process requiring the sequential recruitment of the small GTPases Rab5 and Rab7. These axonal carriers are also used by clostridial neurotoxins and neurotrophins (26, 54), as well as poliovirus (55), and may represent a common organelle providing a protective environment responsible for long-range transport in neurons (1). We also showed that CAR, the docking molecule of CAV-2 (56, 57), was found in endosomes together with CAV-2, suggesting that it used CAR to access the CNS (8).

As a virus receptor, the role of CAR was mainly considered as a docking platform, with no primordial function described in internalization. Typically, it is thought that some AdVs use CAR to dock, followed by integrin-mediated internalization. This is supported by data showing that deletion of the intracellular tail of CAR still allowed AdV-mediated transduction (6).

Viral Ligands Induce CAR Endocytosis

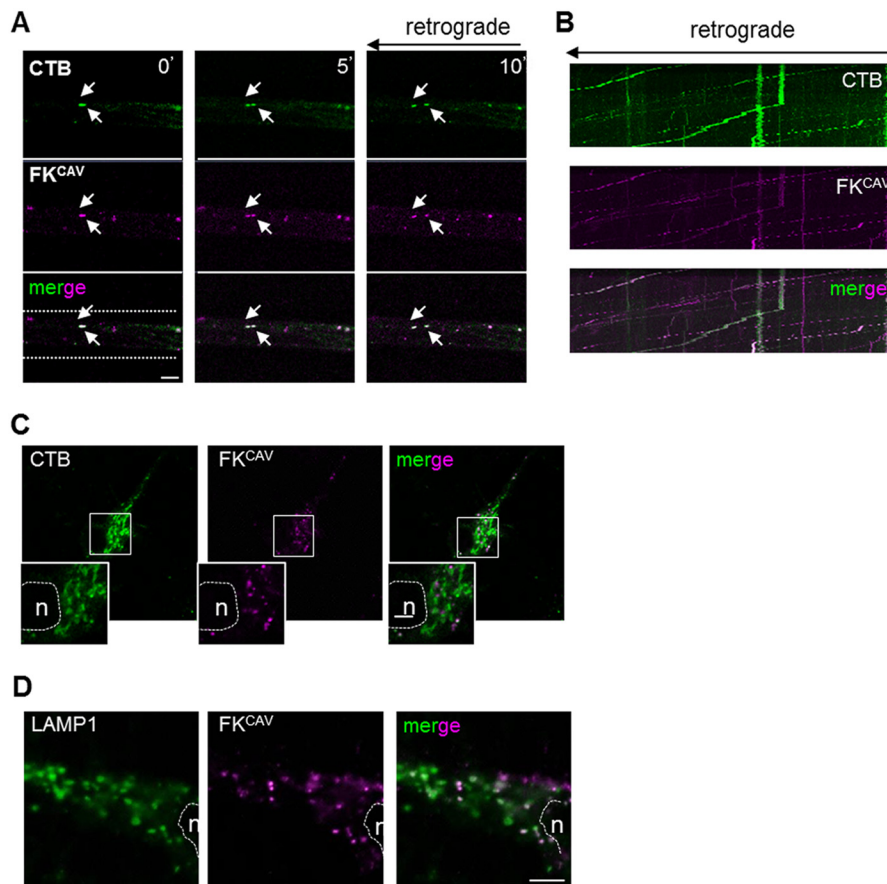


FIGURE 8. CAR and CTB co-transport and sorting after axonal retrograde transport. A–C, FK^{CAV}/CAR were co-transported with CTB in axonal carriers. A, hippocampal neurons cultured in MCs were incubated with Cy5-FK^{CAV} and Alexa 488-CTB in the axonal compartment for 60 min at 37 °C and then imaged in the microgrooves. Still frames of a movie show Cy5-FK^{CAV} and Alexa 488-CTB in the same axonal carriers undergoing retrograde transport. Arrows show moving compartments positive for both ligands (co-transport of 75% ± 9%; *n* = 3, 94 structures were counted; results are expressed as mean ± S.E.). B, kymographs show similar profiles of transported Cy5-FK^{CAV} and Alexa 488-CTB. C, CTB and CAR were sorted differently after axonal transport. Hippocampal neurons cultured in MCs were incubated with Cy5-FK^{CAV} and Alexa 488-CTB in the axonal compartment for 3 h at 37 °C, and imaged in the cell body compartment. Dashed line and *n* identify the nucleus. Insets show minimal colocalization between FK^{CAV} and CTB. D, CAR was targeted to lysosomes after axonal transport. Hippocampal neurons cultured in MCs were incubated with Cy5-FK^{CAV} in the axonal compartment for 3 h at 37 °C, fixed, stained for the lysosomal marker LAMP1, and imaged at the cell body compartment. Numerous FK^{CAV}-positive structures contain LAMP1 (88% ± 3%; *n* = three independent experiments, 140 structures were counted. Results are expressed as mean ± S.E.). Dashed line and *n* identify the nucleus. Scale bars, 5 μm.

Similarly, during CVB endocytosis in polarized epithelial cells CAR remained at the plasma membrane, whereas CVB was internalized (7). However, we previously showed that FK^{CAV} triggered efficient CAR axonal transport, demonstrating that CAR could be directly linked to an endocytic pathway in motor neurons (8). We have now shown that CAV-2 and FK^{CAV} triggered CAR internalization in different neuronal types and cell lines. Moreover, unlike that reported in other cell types, HAdV5 also triggered CAR internalization in neurons. As CAR engagement can regulate signaling pathways (10, 11), it is conceivable that CAR plays a yet undescribed role in endocytosis of AdVs and/or signaling cascades affecting AdV propagation in some cell types. Whether the neuronal signaling of CAR is pro- or antiviral is obviously unknown.

Notably, we show that not all CAR “ligands” behaved similarly. Antibodies directed against the extracellular D1 and D2 domains did not lead to CAR internalization, whereas FK^{CAV}, CAV-2, and HAdV5 did. CAR can form homodimers in *trans* and in *cis* (18, 19, 28). The binding sites and affinity of viral and non-viral ligands have been measured and could explain why we observed differences in terms of ligand-induced internaliza-

tion. Indeed, FK^{CAV}, as a trimer, is theoretically able to engage three CAR molecules (9, 58), whereas CAV-2 and HAdV5 have 12 trimeric fibers and therefore are, in theory, able to engage 36 CAR monomers. Moreover, it is worth considering that the CAR-binding affinity of these ligands could also regulate its membrane trafficking: notably, FK^{CAV} binds to CAR with a lower *K_d* than FK^{HAdV5} (1.1 versus 7.9 nM) (9, 59). Similarly, FK-CAR affinity is higher than the CAR D1-D1 homotypic interaction (*K_d* 16 μM) (60). Excess fiber production during HAdV5 propagation may perturb CAR-CAR homotypic interaction, as it binds similar residues in the D1 domain, and disrupts tight junctions during AdV epithelial infection (28).

The hypothesis we favor for ligand-induced CAR internalization is that CAR-CAR interaction needs to be displaced, as during FK^{CAV} or AdV engagement: it would not be clustering, but disengagement that triggers CAR internalization. In support of this view, polyclonal anti-CAR antibodies, in conditions that mimic multimeric ligand engagement, did not induce CAR endocytosis. We postulate that disruption of the CAR-CAR interaction then favors, or unmasks, intra- or intermolecular interactions that will induce endocytosis. This, coupled to

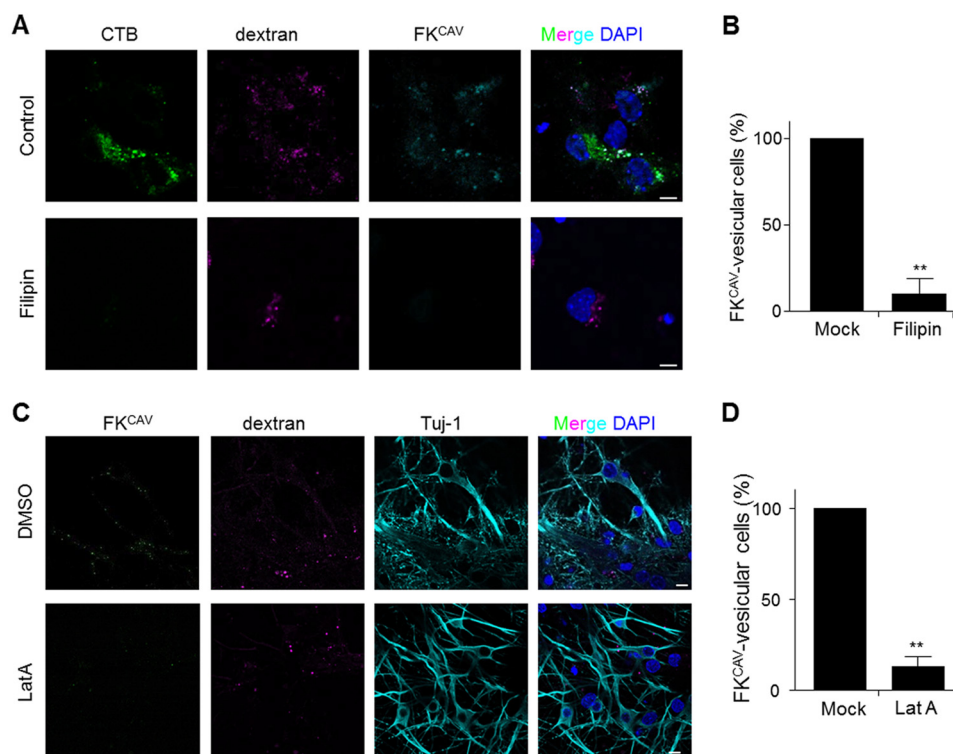


FIGURE 9. Lipid raft- and actin-dependent CAR axonal endocytosis. *A*, cholesterol sequestration disrupted CAR axonal retrograde transport. Hippocampal neurons cultured in MCs for 8 DIV were treated for 30 min with 5 $\mu\text{g}/\text{ml}$ of filipin in the axonal compartment and ligands (Alexa 488-CTB, Cy5-FK^{CAV}, and rhodamine/dextran) were applied to the axonal compartment. Axonal transport was allowed for 3 h at 37 °C. Filipin-treated and control (dimethyl sulfoxide, DMSO) cells transported the fluid-phase marker dextran, but lipid microdomain receptors (GM1 and CAR) could not be transported back to cell bodies. *B*, quantification of filipin effect on FK^{CAV} retrograde transport ($n =$ three independent experiments, 5 fields were quantified for each experiment and each condition; results are expressed as mean \pm S.E. compared with control cells set as 100%). *C*, actin disassembly inhibited CAR axonal retrograde transport. Hippocampal neurons cultured in MCs for 8 DIV were treated for 2 h with LatA (10 μM) in the axonal compartment and ligands (Cy5-FK^{CAV} and rhodamine/dextran) were applied to the axonal compartment. Axonal transport was allowed for 3 h at 37 °C, cells were fixed and stained with β 3-tubulin (*Tuj-1*). LatA-treated cells transported the fluid-phase marker dextran, but not FK^{CAV}. *D*, quantification of the LatA effect on FK^{CAV} retrograde transport ($n =$ three independent experiments, 5 fields were quantified for each experiment and each condition; results are expressed as mean \pm S.E. compared with control cells set as 100%. **, p value <0.01 versus control). Scale bars: *A*, 5 μm ; *B*, 10 μm .

amino acids between 261 and 274, could induce signals necessary for CAR entry (Fig. 11). Interestingly, CAR-binding CVB do not bind at the D1–D1 interface, but to residues situated on the side of the D1 domain (61). This observation is consistent with our hypothesis and why CAR would not be endocytosed during CVB entry in epithelial cells (7, 31). As viruses have been selected for their ability to structurally mimic endogenous host ligands (62), it is likely that a CAR ligand could trigger CAR-CAR disengagement and subsequent internalization. Interestingly, junctional adhesion molecule type L and AdVs bind similar domains on CAR with an affinity higher than CAR-CAR interaction (K_d 5 versus 16 μM) to elicit signaling (10). However, the junctional adhesion molecule type L-CAR interaction occurs in *trans* and was not reported to trigger CAR internalization.

We found that CAR is recruited to cholesterol-rich microdomains in neurons. In contrast to EGFR, which exits lipid microdomains prior to endocytosis, CAR location was maintained during ligand-induced entry. Furthermore, the integrity of lipid microdomains was necessary for CAR endocytosis. Lipid microdomain-mediated entry is a general term to describe cholesterol-dependent mechanisms. However, lipid microdomains are heterogeneous by nature and can differ in terms of composition and size (63, 64). Caveolin-mediated

entry is probably the best described lipid microdomain-mediated endocytic pathway. However, although neurons express caveolin (65), there is no evidence that caveolae can form in neurons (66), which would exclude this endocytic route in CAR internalization. Flotillin-dependent entry is another cholesterol-dependent pathway. In neurons, flotillin-1 can regulate the endocytosis of several proteins including the amyloid precursor protein (67) and semaphorin 3A (68). Our data does not exclude the possibility that CAR could enter via this pathway.

Because the intracellular domain of CAR has a potential AP2 binding site, we also tested the involvement of clathrin and dynamin in the internalization of CAV-2. This site has been well characterized in the basolateral sorting of CAR through AP1 in epithelial cells, but its role in endocytosis was recently questioned (36, 69). Using deletion mutants lacking this site and overexpression of a dominant-negative AP2 mutant, we showed that CAR was still efficiently endocytosed following FK^{CAV} engagement, suggesting that clathrin had a nonessential role in this process. Perturbation of dynamin function and actin depolymerization, however, inhibited CAR internalization. Clathrin-independent, dynamin- and lipid microdomain-mediated endocytosis has been previously reported for cholera toxin (70), SV40 (71), and proteoglycan (72). Actin plays major roles in numerous internalization pathways (40), but its

Viral Ligands Induce CAR Endocytosis

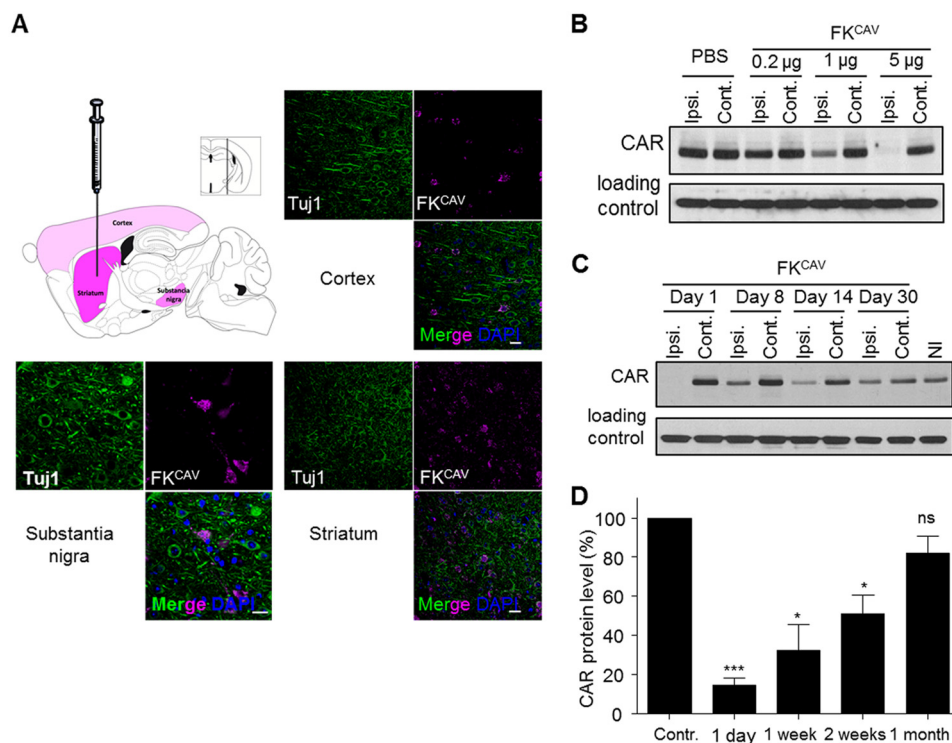


FIGURE 10. CAR is transported and degraded *in vivo*. *A*, intraparenchymal injections of FK^{CAV} led to its axonal transport in connected regions. Scheme of brain regions showing Cy5-FK^{CAV} localization after injection in the striatum. Slices were stained for β 3-tubulin (*Tuj-1*). *B* and *C*, injection of 5 μ g of FK^{CAV} led to CAR degradation in the striatum. Representative immunoblots of at least three independent experiments show CAR expression in the mouse striatum. *B*, CAR levels 1 day post-injection of PBS or different doses of FK^{CAV}. A dose effect of FK^{CAV} injection on CAR expression was observed. *C*, time course effect of FK^{CAV} injection on CAR expression. CAR levels were restored one month post-injection (*Ipsi.*, ipsilateral; *Cont.*, contralateral; *NI.*, non-injected). *D*, quantification of three independent experiments; results are expressed as mean \pm S.E. compared with control set as 100%. *, *p* value <0.05; ***, *p* value <0.001 versus control). Scale bars, 20 μ m.

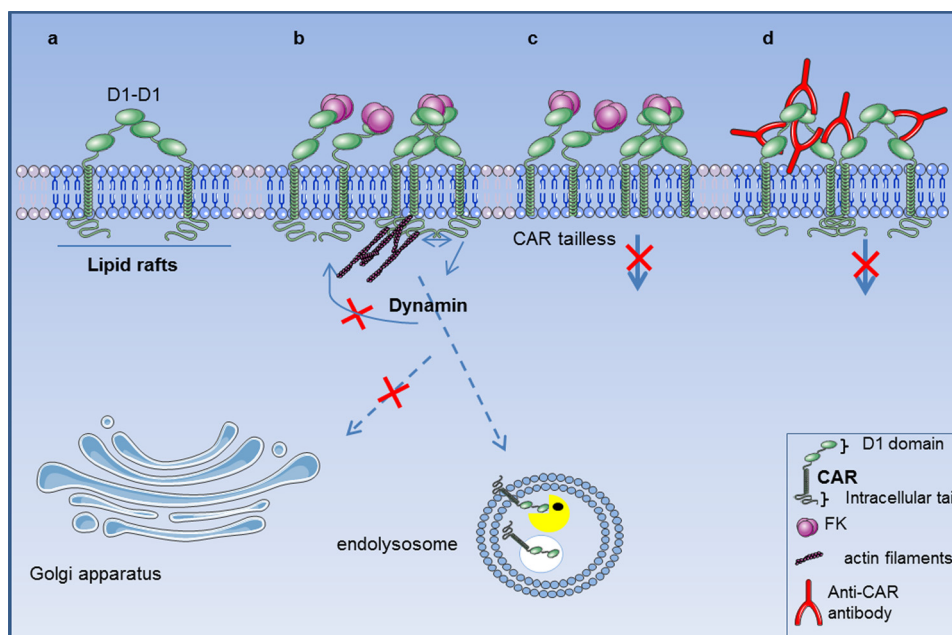


FIGURE 11. Mechanisms of ligand-induced CAR endocytosis in neuronal cells. *a*, CAR (in green) is located in lipid rafts (in blue) and homodimeric interaction occurs through the D1 domain. *b*, the trimeric fiber knob (FK^{CAV}, in magenta), the CAR-interacting domain of some adenovirus types, binds with higher affinity to the D1-D1 interacting site and triggers D1-D1 disengagement. FK^{CAV} can engage one, two, or three CAR molecules leading to either clustering, or D1 disengagement in FK^{CAV} saturating conditions. Lipid raft integrity, dynamin, and actin (in purple) play crucial roles in subsequent internalization that will target CAR to endolysosomes for degradation (lysosomal enzymes represented by yellow Pacman). *c*, a region (amino acids 261–274) in the tail of CAR was essential for ligand-induced CAR endocytosis. *d*, clustering through antibody (in red) or coxsackievirus (7) binding, was insufficient to trigger CAR internalization, likely because they do not disrupt D1-D1 interactions and therefore do not favor or unmask, intra- or intermolecular interactions that regulate ligand-induced CAR endocytosis.

involvement in mammalian endocytosis remains controversial. Its role is best studied during clathrin-mediated endocytosis, but other routes also require actin dynamics, such as macropinocytosis and lipid-dependent entry (40). The analogy with SV40 and GM1-mediated internalization is pertinent, as SV40 also uses dynamin and lipid microdomains and also actin during entry (71). It was suggested that viral diffusion at the plasma membrane is blocked by actin assembly leading to its immobilization in lipid microdomains (73). Indeed, the formation of cholesterol-sensitive clusters may be regulated by cortical actin (74). CAR drifting at the plasma membrane has also been reported and was influenced by the actin cytoskeleton (75). Notably, actin interacts with the CAR cytoplasmic domain (41). Whether this interaction and its role in the regulation of CAR lateral diffusion at the plasma membrane are necessary for CAR endocytosis remain to be tested.

After FK^{CAV} engagement *ex vivo* and *in vivo*, the majority of CAR was not recycled or transported to the Golgi network, but targeted to lysosomes for degradation. CTB and FK^{CAV} shared a common axonal carrier, but differed in their final destination, suggesting that a general endocytic pathway was responsible for long-range transport and that somatodendritic sorting selectively targeted ligand-receptor complexes to distinct locations. As the transition from axon to soma after retrograde transport is still poorly understood, using these ligands may be of help to understand the nature of the endocytic compartments responsible for sorting.

Besides its role in AdV entry, what could CAR depletion from the plasma membrane, and targeting, for degradation, do to its neuronal function? As CAR is also coupled to signaling pathways (e.g. Ref. 11), one possibility is that its ligand-mediated degradation regulates mechanisms important for neuronal homeostasis such as migration or survival. Indeed, a potential role in neurite outgrowth has been postulated (18). In neurons, receptor-induced internalization following ligand binding is well described for nerve growth factor and TrkA where different signals are generated at the plasma membrane and in endosomes (76). Similarly, endocytosis at growth cones during development allows endosomes containing nerve growth factor, TrkA, and downstream signaling molecules to be transported to the cell body to trigger a transcriptional response necessary for survival (15). Moreover, CAMs can also be internalized to promote local and distal signaling, membrane remodeling, and to modulate the adhesive properties (17, 77). For example, fibronectin triggers integrin internalization and targeting to lysosomes to control cellular migration (16). Likewise, L1CAM is depleted from the plasma membrane to regulate axonal growth (17, 78) and can be degraded by the lysosomal system (79). This highlights the role of lysosomes in signal termination. It will also be particularly relevant to determine whether ligand-induced CAR endocytosis and degradation are associated with signal activation and the endogenous function of CAR in the CNS as was reported for other CAMs.

In conclusion, we describe the mechanisms behind ligand-induced CAR endocytosis in neurons. Characterizing how CAR interacts with molecules regulating internalization and the endocytic machinery may also help to better understand how

pathogens access the CNS and how cell adhesion molecules convey signals necessary for neuronal homeostasis.

Acknowledgments—We thank the IGMM Animal Facility and Montpellier Rio Imaging for microscopy studies and Thierry Gostan for help with statistical analyses.

REFERENCES

- Salinas, S., Schiavo, G., and Kremer, E. J. (2010) A hitchhiker's guide to the nervous system. The complex journey of viruses and toxins. *Nat. Rev. Microbiol.* **8**, 645–655
- Salinas, S., Bilsland, L. G., and Schiavo, G. (2008) Molecular landmarks along the axonal route. Axonal transport in health and disease. *Curr. Opin. Cell Biol.* **20**, 445–453
- Franker, M. A., and Hoogenraad, C. C. (2013) Microtubule-based transport. Basic mechanisms, traffic rules and role in neurological pathogenesis. *J. Cell Sci.* **126**, 2319–2329
- Koyuncu, O. O., Hogue, I. B., and Enquist, L. W. (2013) Virus infections in the nervous system. *Cell Host Microbe* **13**, 379–393
- Freimuth, P., Philipson, L., and Carson, S. D. (2008) The coxsackievirus and adenovirus receptor. *Curr. Top. Microbiol. Immunol.* **323**, 67–87
- Wang, X., and Bergelson, J. M. (1999) Coxsackievirus and adenovirus receptor cytoplasmic and transmembrane domains are not essential for coxsackievirus and adenovirus infection. *J. Virol.* **73**, 2559–2562
- Coyne, C. B., and Bergelson, J. M. (2006) Virus-induced Abl and Fyn kinase signals permit coxsackievirus entry through epithelial tight junctions. *Cell* **124**, 119–131
- Salinas, S., Bilsland, L. G., Henaff, D., Weston, A. E., Keriell, A., Schiavo, G., and Kremer, E. J. (2009) CAR-associated vesicular transport of an adenovirus in motor neuron axons. *PLoS Pathog.* **5**, e1000442
- Seiradake, E., Lortat-Jacob, H., Billet, O., Kremer, E. J., and Cusack, S. (2006) Structural and mutational analysis of human Ad37 and canine adenovirus 2 fiber heads in complex with the D1 domain of coxsackie and adenovirus receptor. *J. Biol. Chem.* **281**, 33704–33716
- Verdino, P., Witherden, D. A., Havran, W. L., and Wilson, I. A. (2010) The molecular interaction of CAR and JAML recruits the central cell signal transducer PI3K. *Science* **329**, 1210–1214
- Tamanini, A., Nicolis, E., Bonizzato, A., Bezzerri, V., Melotti, P., Assael, B. M., and Cabrini, G. (2006) Interaction of adenovirus type 5 fiber with the coxsackievirus and adenovirus receptor activates inflammatory response in human respiratory cells. *J. Virol.* **80**, 11241–11254
- Xie, J., Chiang, L., Contreras, J., Wu, K., Garner, J. A., Medina-Kauwe, L., and Hamm-Alvarez, S. F. (2006) Novel fiber-dependent entry mechanism for adenovirus serotype 5 in lacrimal acini. *J. Virol.* **80**, 11833–11851
- Schaefer, A. W., Kamiguchi, H., Wong, E. V., Beach, C. M., Landreth, G., and Lemmon, V. (1999) Activation of the MAPK signal cascade by the neural cell adhesion molecule L1 requires L1 internalization. *J. Biol. Chem.* **274**, 37965–37973
- Gonnord, P., Blouin, C. M., and Lamaze, C. (2012) Membrane trafficking and signaling. Two sides of the same coin. *Semin. Cell Dev. Biol.* **23**, 154–164
- Ibáñez, C. F. (2007) Message in a bottle. Long-range retrograde signaling in the nervous system. *Trends Cell Biol.* **17**, 519–528
- Lobert, V. H., Brech, A., Pedersen, N. M., Wesche, J., Oppelt, A., Malerød, L., and Stenmark, H. (2010) Ubiquitination of $\alpha 5\beta 1$ integrin controls fibroblast migration through lysosomal degradation of fibronectin-integrin complexes. *Dev. Cell* **19**, 148–159
- Castellani, V., Falk, J., and Rougon, G. (2004) Semaphorin3A-induced receptor endocytosis during axon guidance responses is mediated by L1 CAM. *Mol. Cell Neurosci.* **26**, 89–100
- Patzke, C., Max, K. E., Behlke, J., Schreiber, J., Schmidt, H., Dorner, A. A., Kröger, S., Henning, M., Otto, A., Heinemann, U., and Rathjen, F. G. (2010) The coxsackievirus-adenovirus receptor reveals complex homophilic and heterophilic interactions on neural cells. *J. Neurosci.* **30**, 2897–2910
- Farmer, C., Morton, P. E., Snippe, M., Santis, G., and Parsons, M. (2009)

- Coxsackie adenovirus receptor (CAR) regulates integrin function through activation of p44/42 MAPK. *Exp. Cell Res.* **315**, 2637–2647
20. Ezratty, E. J., Bertaux, C., Marcantonio, E. E., and Gundersen, G. G. (2009) Clathrin mediates integrin endocytosis for focal adhesion disassembly in migrating cells. *J. Cell Biol.* **187**, 733–747
 21. Granseth, B., Odermatt, B., Royle, S. J., and Lagnado, L. (2006) Clathrin-mediated endocytosis is the dominant mechanism of vesicle retrieval at hippocampal synapses. *Neuron* **51**, 773–786
 22. Kremer, E. J., Boutin, S., Chillon, M., and Danos, O. (2000) Canine adenovirus vectors. An alternative for adenovirus-mediated gene transfer. *J. Virol.* **74**, 505–512
 23. Hnasko, T. S., Perez, F. A., Scouras, A. D., Stoll, E. A., Gale, S. D., Luquet, S., Phillips, P. E., Kremer, E. J., and Palmiter, R. D. (2006) Cre recombinase-mediated restoration of nigrostriatal dopamine in dopamine-deficient mice reverses hypophagia and bradykinesia. *Proc. Natl. Acad. Sci. U.S.A.* **103**, 8858–8863
 24. Persaud-Sawin, D. A., Lightcap, S., and Harry, G. J. (2009) Isolation of rafts from mouse brain tissue by a detergent-free method. *J. Lipid Res.* **50**, 759–767
 25. Taylor, A. M., Rhee, S. W., and Jeon, N. L. (2006) Microfluidic chambers for cell migration and neuroscience research. *Methods Mol. Biol.* **321**, 167–177
 26. Restani, L., Giribaldi, F., Manich, M., Bercsenyi, K., Menendez, G., Rossetto, O., Caleo, M., and Schiavo, G. (2012) Botulinum neurotoxins A and E undergo retrograde axonal transport in primary motor neurons. *PLoS Pathog.* **8**, e1003087
 27. Soudais, C., Laplace-Builhe, C., Kissa, K., and Kremer, E. J. (2001) Preferential transduction of neurons by canine adenovirus vectors and their efficient retrograde transport *in vivo*. *FASEB J.* **15**, 2283–2285
 28. Walters, R. W., Freimuth, P., Moninger, T. O., Ganske, I., Zabner, J., and Welsh, M. J. (2002) Adenovirus fiber disrupts CAR-mediated intercellular adhesion allowing virus escape. *Cell* **110**, 789–799
 29. Lingwood, D., and Simons, K. (2010) Lipid rafts as a membrane-organizing principle. *Science* **327**, 46–50
 30. Ashbourne Excoffon, K. J., Moninger, T., and Zabner, J. (2003) The coxsackie B virus and adenovirus receptor resides in a distinct membrane microdomain. *J. Virol.* **77**, 2559–2567
 31. Takahashi, T., and Suzuki, T. (2011) Function of membrane rafts in viral lifecycles and host cellular response. *Biochem. Res. Int.* **2011**, 245090
 32. Wickham, T. J., Mathias, P., Cheresch, D. A., and Nemerow, G. R. (1993) Integrins $\alpha\beta 3$ and $\alpha\beta 5$ promote adenovirus internalization but not virus attachment. *Cell* **73**, 309–319
 33. Mineo, C., Gill, G. N., and Anderson, R. G. (1999) Regulated migration of epidermal growth factor receptor from caveolae. *J. Biol. Chem.* **274**, 30636–30643
 34. Sarnataro, D., Caputo, A., Casanova, P., Puri, C., Paladino, S., Tivodar, S. S., Campana, V., Tacchetti, C., and Zurzolo, C. (2009) Lipid rafts and clathrin cooperate in the internalization of PrP in epithelial FRT cells. *PLoS ONE* **4**, e5829
 35. Meier, O., and Greber, U. F. (2003) Adenovirus endocytosis. *J. Gene Med.* **5**, 451–462
 36. Carvajal-Gonzalez, J. M., Gravotta, D., Mattera, R., Diaz, F., Perez Bay, A., Roman, A. C., Schreiner, R. P., Thuenauer, R., Bonifacino, J. S., and Rodriguez-Boulan, E. (2012) Basolateral sorting of the coxsackie and adenovirus receptor through interaction of a canonical YXX ϕ motif with the clathrin adaptors AP-1A and AP-1B. *Proc. Natl. Acad. Sci. U.S.A.* **109**, 3820–3825
 37. Olusanya, O., Andrews, P. D., Swedlow, J. R., and Smythe, E. (2001) Phosphorylation of threonine 156 of the mu2 subunit of the AP2 complex is essential for endocytosis *in vitro* and *in vivo*. *Curr. Biol.* **11**, 896–900
 38. Ferguson, S. M., and De Camilli, P. (2012) Dynamin, a membrane-remodelling GTPase. *Nat. Rev. Mol. Cell Biol.* **13**, 75–88
 39. Damke, H., Baba, T., Warnock, D. E., and Schmid, S. L. (1994) Induction of mutant dynamin specifically blocks endocytic coated vesicle formation. *J. Cell Biol.* **127**, 915–934
 40. Mooren, O. L., Galletta, B. J., and Cooper, J. A. (2012) Roles for actin assembly in endocytosis. *Annu. Rev. Biochem.* **81**, 661–686
 41. Huang, K. C., Yasruel, Z., Guérin, C., Holland, P. C., and Nalbantoglu, J. (2007) Interaction of the Coxsackie and adenovirus receptor (CAR) with the cytoskeleton. Binding to actin. *FEBS Lett.* **581**, 2702–2708
 42. Orlandi, P. A., and Fishman, P. H. (1998) Filipin-dependent inhibition of cholera toxin. Evidence for toxin internalization and activation through caveolae-like domains. *J. Cell Biol.* **141**, 905–915
 43. Taylor, A. M., Blurton-Jones, M., Rhee, S. W., Cribbs, D. H., Cotman, C. W., and Jeon, N. L. (2005) A microfluidic culture platform for CNS axonal injury, regeneration and transport. *Nat. Methods* **2**, 599–605
 44. Richart, S. M., Simpson, S. A., Kruppenacher, C., Whitbeck, J. C., Pizer, L. I., Cohen, G. H., Eisenberg, R. J., and Wilcox, C. L. (2003) Entry of herpes simplex virus type 1 into primary sensory neurons *in vitro* is mediated by Nectin-1/HveC. *J. Virol.* **77**, 3307–3311
 45. Ohka, S., Matsuda, N., Tohyama, K., Oda, T., Morikawa, M., Kuge, S., and Nomoto, A. (2004) Receptor (CD155)-dependent endocytosis of poliovirus and retrograde axonal transport of the endosome. *J. Virol.* **78**, 7186–7198
 46. Huang, Y. C., Huang, S. L., Chen, S. P., Huang, Y. L., Huang, C. G., Tsao, K. C., and Lin, T. Y. (2013) Adenovirus infection associated with central nervous system dysfunction in children. *J. Clin. Virol.* **57**, 300–304
 47. de Ory, F., Avellón, A., Echevarría, J. E., Sánchez-Seco, M. P., Trallero, G., Cabrerizo, M., Casas, I., Pozo, F., Fedele, G., Vicente, D., Pena, M. J., Moreno, A., Niubo, J., Rabella, N., Rubio, G., Pérez-Ruiz, M., Rodríguez-Iglesias, M., Gimeno, C., Eiros, J. M., Melón, S., Blasco, M., López-Miragaya, I., Varela, E., Martínez-Sapiña, A., Rodríguez, G., Marcos, M. Á., Gegúndez, M. I., Cilla, G., Gabilondo, I., Navarro, J. M., Torres, J., Aznar, C., Castellanos, A., Guisasola, M. E., Negredo, A. I., Tenorio, A., and Vázquez-Morón, S. (2013) Viral infections of the central nervous system in Spain. A prospective study. *J. Med. Virol.* **85**, 554–562
 48. Moore, M. L., Brown, C. C., and Spindler, K. R. (2003) T cells cause acute immunopathology and are required for long-term survival in mouse adenovirus type 1-induced encephalomyelitis. *J. Virol.* **77**, 10060–10070
 49. Gralinski, L. E., Ashley, S. L., Dixon, S. D., and Spindler, K. R. (2009) Mouse adenovirus type 1-induced breakdown of the blood-brain barrier. *J. Virol.* **83**, 9398–9410
 50. Kosulin, K., Haberler, C., Hainfellner, J. A., Amann, G., Lang, S., and Lion, T. (2007) Investigation of adenovirus occurrence in pediatric tumor entities. *J. Virol.* **81**, 7629–7635
 51. Le Gal La Salle, G., Robert, J. J., Berrard, S., Ridoux, V., Stratford-Perricaudet, L. D., Perricaudet, M., and Mallet, J. (1993) An adenovirus vector for gene transfer into neurons and glia in the brain. *Science* **259**, 988–990
 52. Akli, S., Caillaud, C., Vigne, E., Stratford-Perricaudet, L. D., Poenaru, L., Perricaudet, M., Kahn, A., and Peschanski, M. R. (1993) Transfer of a foreign gene into the brain using adenovirus vectors. *Nat. Genet.* **3**, 224–228
 53. Bru, T., Salinas, S., and Kremer, E. (2010) An update on canine adenovirus type 2 and its vectors. *Viruses* **2**, 2134–2153
 54. Deinhardt, K., Salinas, S., Verastegui, C., Watson, R., Worth, D., Hanrahan, S., Buccì, C., and Schiavo, G. (2006) Rab5 and Rab7 control endocytic sorting along the axonal retrograde transport pathway. *Neuron* **52**, 293–305
 55. Ohka, S., Sakai, M., Bohnert, S., Igarashi, H., Deinhardt, K., Schiavo, G., and Nomoto, A. (2009) Receptor-dependent and -independent axonal retrograde transport of poliovirus in motor neurons. *J. Virol.* **83**, 4995–5004
 56. Soudais, C., Boutin, S., Hong, S. S., Chillon, M., Danos, O., Bergelson, J. M., Boulanger, P., and Kremer, E. J. (2000) Canine adenovirus type 2 attachment and internalization. Coxsackievirus-adenovirus receptor, alternative receptors, and an RGD-independent pathway. *J. Virol.* **74**, 10639–10649
 57. Chillon, M., and Kremer, E. J. (2001) Trafficking and propagation of canine adenovirus vectors lacking a known integrin-interacting motif. *Hum. Gene Ther.* **12**, 1815–1823
 58. Lortat-Jacob, H., Chouin, E., Cusack, S., and van Raaij, M. J. (2001) Kinetic analysis of adenovirus fiber binding to its receptor reveals an avidity mechanism for trimeric receptor-ligand interactions. *J. Biol. Chem.* **276**, 9009–9015
 59. Schoehn, G., El Bakkouri, M., Fabry, C. M., Billet, O., Estrozi, L. F., Le, L., Curiel, D. T., Kajava, A. V., Ruigrok, R. W., and Kremer, E. J. (2008) Three-dimensional structure of canine adenovirus serotype 2 capsid. *J. Virol.* **82**,

- 3192–3203
60. van Raaij, M. J., Chouin, E., van der Zandt, H., Bergelson, J. M., and Cusack, S. (2000) Dimeric structure of the coxsackievirus and adenovirus receptor D1 domain at 1.7-Å resolution. *Structure Fold Des.* **8**, 1147–1155
 61. He, Y., Chipman, P. R., Howitt, J., Bator, C. M., Whitt, M. A., Baker, T. S., Kuhn, R. J., Anderson, C. W., Freimuth, P., and Rossmann, M. G. (2001) Interaction of coxsackievirus B3 with the full-length coxsackievirus-adenovirus receptor. *Nat. Struct. Biol.* **8**, 874–878
 62. Drayman, N., Glick, Y., Ben-nun-shaul, O., Zer, H., Zlotnick, A., Gerber, D., Schueler-Furman, O., and Oppenheim, A. (2013) Pathogens use structural mimicry of native host ligands as a mechanism for host receptor engagement. *Cell Host Microbe* **14**, 63–73
 63. Rajendran, L., and Simons, K. (2005) Lipid rafts and membrane dynamics. *J. Cell Sci.* **118**, 1099–1102
 64. Simons, K., and Gerl, M. J. (2010) Revitalizing membrane rafts. New tools and insights. *Nat. Rev. Mol. Cell Biol.* **11**, 688–699
 65. Boulware, M. I., Kordasiewicz, H., and Mermelstein, P. G. (2007) Caveolin proteins are essential for distinct effects of membrane estrogen receptors in neurons. *J. Neurosci.* **27**, 9941–9950
 66. Lang, D. M., Lommel, S., Jung, M., Ankerhold, R., Petrausch, B., Laessing, U., Wiechers, M. F., Plattner, H., and Stuermer, C. A. (1998) Identification of reggie-1 and reggie-2 as plasmamembrane-associated proteins which cocluster with activated GPI-anchored cell adhesion molecules in non-caveolar micropatches in neurons. *J. Neurobiol.* **37**, 502–523
 67. Schneider, A., Rajendran, L., Honsho, M., Gralle, M., Donnert, G., Wouters, F., Hell, S. W., and Simons, M. (2008) Flotillin-dependent clustering of the amyloid precursor protein regulates its endocytosis and amyloidogenic processing in neurons. *J. Neurosci.* **28**, 2874–2882
 68. Carcea, I., Ma'ayan, A., Mesias, R., Sepulveda, B., Salton, S. R., and Benson, D. L. (2010) Flotillin-mediated endocytic events dictate cell type-specific responses to semaphorin 3A. *J. Neurosci.* **30**, 15317–15329
 69. Diaz, F., Gravotta, D., Deora, A., Schreiner, R., Schoggins, J., Falck-Pedersen, E., and Rodriguez-Boulan, E. (2009) Clathrin adaptor AP1B controls adenovirus infectivity of epithelial cells. *Proc. Natl. Acad. Sci. U.S.A.* **106**, 11143–11148
 70. Lajoie, P., Kojic, L. D., Nim, S., Li, L., Dennis, J. W., and Nabi, I. R. (2009) Caveolin-1 regulation of dynamin-dependent, raft-mediated endocytosis of cholera toxin-B subunit occurs independently of caveolae. *J. Cell. Mol. Med.* **13**, 3218–3225
 71. Pelkmans, L., Püntener, D., and Helenius, A. (2002) Local actin polymerization and dynamin recruitment in SV40-induced internalization of caveolae. *Science* **296**, 535–539
 72. Payne, C. K., Jones, S. A., Chen, C., and Zhuang, X. (2007) Internalization and trafficking of cell surface proteoglycans and proteoglycan-binding ligands. *Traffic* **8**, 389–401
 73. Ewers, H., and Helenius, A. (2011) Lipid-mediated endocytosis. *Cold Spring Harb. Perspect. Biol.* **3**, a004721
 74. Goswami, D., Gowrishankar, K., Bilgrami, S., Ghosh, S., Raghupathy, R., Chadda, R., Vishwakarma, R., Rao, M., and Mayor, S. (2008) Nanoclusters of GPI-anchored proteins are formed by cortical actin-driven activity. *Cell* **135**, 1085–1097
 75. Burckhardt, C. J., Suomalainen, M., Schoenenberger, P., Boucke, K., Hemmi, S., and Greber, U. F. (2011) Drifting motions of the adenovirus receptor CAR and immobile integrins initiate virus uncoating and membrane lytic protein exposure. *Cell Host Microbe* **10**, 105–117
 76. Zhang, Y., Moheban, D. B., Conway, B. R., Bhattacharyya, A., and Segal, R. A. (2000) Cell surface Trk receptors mediate NGF-induced survival while internalized receptors regulate NGF-induced differentiation. *J. Neurosci.* **20**, 5671–5678
 77. Sakisaka, T., and Takai, Y. (2005) Cell adhesion molecules in the CNS. *J. Cell Sci.* **118**, 5407–5410
 78. Kamiguchi, H., and Yoshihara, F. (2001) The role of endocytic I1 trafficking in polarized adhesion and migration of nerve growth cones. *J. Neurosci.* **21**, 9194–9203
 79. Schäfer, M. K., Schmitz, B., and Diestel, S. (2010) L1CAM ubiquitination facilitates its lysosomal degradation. *FEBS Lett.* **584**, 4475–4480
 80. Paxinos, G., and Franklin, K. B. J. (2003) *The Mouse Brain in Stereotaxic Coordinates*, 2nd Ed., pp. 22 and 30, Academic Press, San Diego, CA